1	
2	
3	
4	Soil pore architecture and rhizosphere legacy define N2O
5	production in root detritusphere
6	
7	
8	
9	
10	
11	Kyungmin Kim ^{1,2} , Jenie Gil ^{2,3} , Nathaniel E. Ostrom ^{2,3} , Hasand Gandhi ^{2,3} , Maxwell S. Oerther ^{1,2}
12	Yakov Kuzyakov ^{4,5} , Andrey K. Guber ^{1,2} , and Alexandra N. Kravchenko ^{1,2}
13	¹ Department of Plant Soil and Microbial Sciences, Michigan State University, MI, U.S.A
14	² DOE Great Lakes Bioenergy Research Center, Michigan State University, MI, U.S.A
15	³ Department of Integrative Biology, Michigan State University, MI, U.S.A
16 17	⁴ Department of Agricultural Soil Science, Department of Soil Science of Temperate Ecosystems, Georg-August-Universität Göttingen, Göttingen, Germany
18 19	⁵ Agro-Technological Institute, RUDN University, 117198 Moscow, Russia
20	*Electronically submitted to Soil Biology and Biochemistry

Keywords

- 22 Bioenergy, Detritusphere, Switchgrass, Root Decomposition, Nitrous Oxide, Greenhouse Gas
- Emission, ¹³C Pulse Labeling, Zymography, Soil Pore Architecture, ¹⁵N labeling, Microbial
- 24 Hotspots

25

26

21

Highlights

- Rhizosphere soil carries a strong legacy effect as it turns into detritusphere.
- Pore architecture is 6 times more important than soil water content in N₂O emission.
- N₂O emission is most intensive in microbial activity hotspots in large pores.
 - Root- and soil-derived N₂O emissions both occur near decomposing roots.

31

32

30

Abstract

- Root detritusphere is one of the most important sources of N₂O, however, understanding of how
- N₂O emission from the detritusphere is influenced by soil properties remains elusive. Here, we
- evaluated the effects of pore architecture and soil moisture on N₂O emission during the
- decomposition of *in-situ* grown roots of switchgrass, an important bioenergy crop. We combined
- dual isotope labeling (¹³C and ¹⁵N) with zymography to gain insights into the location of the
- microbial N₂O production in soils with contrasting pore architectures. In the studied soil, the
- effect of soil pore architecture on N₂O emissions was 6 times greater than that of soil moisture.
- Soil dominated by \geq 30 µm Ø pores (i.e., large-pore soil) had higher chitinase activity than the
- soil dominated by $\leq 10 \, \mu \text{m} \, \emptyset$ pores (i.e., small-pore soil), especially near the decomposing roots.

The chitinase activity on the decomposing roots was positively correlated with emission of rootderived N₂O, indicating that N released from root decomposition was an important source of N₂O. Greater N₂O and N₂ emission was induced by switchgrass roots in soils dominated by the large- compared to the small-pore soils. The microenvironment developed near decomposing roots of the large-pore soil also resulted in positive N₂O priming. Our study challenged the traditional view on soil moisture as the main factor of N2O production. Production and emission of N₂O was most intensive in microbial activity hotspots (i.e., rhizosphere legacy) in the large pores, where decomposed roots release mineral N as the main N₂O source.

Introduction

62

63

64

65

66

67

68

69

70

71

72

73

74

75

76

77

78

79

80

81

82

83

84

By regulating the availability of O₂, nitrogen, and other nutrients to soil microorganisms, pore architecture and moisture affect environmental conditions within the soil matrix, and, hence, drive production pathways, transport, and emission of N₂O (Bollmann and Conrad, 1998; Butterbach-Bahl et al., 2013; Castellano et al., 2010; Chen et al., 2013). The biological processes of nitrification and denitrification are responsible for most of upland soil N2O production (Bracken et al., 2021; Velthof et al., 2002), although other pathways - including dissimilatory nitrate reduction to ammonium, surface decomposition of ammonium nitrate, biological nitrogen fixation, and chemodenitrification - also can make an impact (Butterbach-Bahl et al., 2013; Morley and Baggs, 2010). The absolute amount of N₂O emission tends to increase along with soil moisture content until 80% WFPS (Schaufler et al., 2010), and as overall soil pore size decreases by compaction (Saggar et al., 2013). As the WFPS increases and pore size decreases, contribution of dinitrogen (N₂), the final denitrification product, grows, reducing the N₂O:N₂ molar ratio (Schaufler et al., 2010; Zaman et al., 2012). Previous source partitioning studies showed nitrification dominating in relatively dry soils, e.g., at soil water-filled pore space (WFPS) of 40~60%, while denitrification gained importance at higher soil water contents, reaching maximum levels at 70~90% WFPS (Bateman and Baggs, 2005; Bracken et al., 2021; Davidson et al., 1986; Ruser et al., 2006; van der Weerden et al., 2012). However, these general rules are not always applicable, in part due to substantial microscale heterogeneity in soil biological activity and O₂ availability, which determine the rates and pathways of microbial processes (Blagodatsky et al., 2011). For example, even in a relatively dry soil, i.e., at 40-60% WFPS, physical constraints of O₂ supply to the center of soil aggregates can lead to formation of anoxic microsites and localized, but sizeable, N₂O production via

denitrification (Schlüter et al., 2018). Likewise, plant residue fragments within a relatively dry soil matrix absorb water from surrounding soil and generate microscale moisture gradients, creating anoxic microenvironments favorable to denitrification (Kim et al., 2020; Kravchenko et al., 2017). Counterintuitively, the influence of such microsites can be enhanced under conditions that are generally considered unfavorable to N₂O production via denitrification, i.e., in coarse textured soils, in soils with well-developed pore architecture dominated by macro-pores (>30 μm Ø), and/or at low soil moisture contents (Kim et al., 2020; Kravchenko et al., 2017; Schlüter et al., 2018). Despite their small spatial extent, such microsites can be responsible for a majority of soil N₂O emissions (Parkin, 1987), limiting the ability to accurately predict and model N₂O emissions (Butterbach-Bahl et al., 2013; Groffman et al., 2009).

Plant roots play a major role in all processes involved in N₂O production and emission. They are the main drivers in the formation of soil pores (Angers and Caron, 1998; Bardgett et al., 2014; Bengough, 2012; Jin et al., 2017) and key sources of organics supporting microbial growth in rhizosphere of live roots and in detritusphere around dead roots (Hu et al., 2016). Impending elevated CO₂ levels and precipitation changes can alter soil pore characteristics (Caplan et al., 2017; Hirmas et al., 2018; Wu et al., 2018), root growth (Hu et al., 2016), root development patterns (Calleja-Cabrera et al., 2020), and root-soil interactions. Mechanistic understanding of joint contributions of plant roots and soil pore architecture to N₂O emissions is integral to predicting and modeling climate change impacts.

We posit that the interactions between decomposing plant roots and soil pores on N₂O production and emission must be studied with roots decomposing at the same locations within the soil matrix where they grew and died. Living roots substantially modify the soil in their vicinity, inducing changes in soil structure (Angers and Caron, 1998; Helliwell et al., 2019;

Koebernick et al., 2017), hydraulic properties (Carminati et al., 2010), microbial community structure and abundance (Berendsen et al., 2012; Bird et al., 2011; Liang et al., 2016), and nutrient level/availability (Dijkstra et al., 2009; Marschner et al., 1987; Meier et al., 2017). Upon roots' death, the microenvironmental conditions within the rhizosphere are inherited by the root detritusphere surrounding decomposing root residues. Detritusphere is as litter-soil interface and a zone of soil affected by litter decomposition (Liu et al., 2011). It is an important hotspot of microbial activity and C and N processing, second only to rhizosphere in the magnitude and spatial extent and exceeding all other types of soil hotspots in the temporal duration of its influence (Kuzyakov and Blagodatskaya, 2015). The microenvironmental conditions within the root detritusphere can be substantially different from that of bulk soil (Kim et al., 2020; Kuzyakov and Razavi, 2019). A common experimental practice in root decomposition studies is to remove root residues from the original soil matrix and to incorporate them into sieved and mixed soil, either as intact layers or as a ground material mixed with the soil. As a result, the influence of the unique features of rhizosphere-inherited microenvironments in the root detritusphere is no longer accounted for. This can result in misleading conclusions because soil characteristics in the detritusphere around an *in-situ* decomposing root are substantially different from the detritusphere around an artificially incorporated root residue. Exploring decomposition of *in-situ* grown roots allows accounting for the rhizosphere legacy effect on N₂O emission during root decomposition. We studied *in-situ* grown root decomposition in a model system of monoculture switchgrass

108

109

110

111

112

113

114

115

116

117

118

119

120

121

122

123

124

125

126

127

128

129

130

(*Panicum Virgatum* L.), a prominent grass of North American prairie and a promising bioenergy feedstock (Gelfand et al., 2020). While N fertilizers are often the main source of N₂O emissions in conventional agriculture (Tian et al., 2019), their role is less conspicuous in bioenergy

switchgrass systems, which typically receive lower N fertilizer inputs than cash crops (Adler et al., 2007). It is partly because switchgrass biomass yields only weakly respond to N availability (Roley et al., 2018; Wang et al., 2019). Rather, decomposing roots are expected to play a major role in N₂O production in switchgrass systems (Adler et al., 2007; Cherubini and Jungmeier, 2010; Monti et al., 2012).

131

132

133

134

135

136

137

138

139

140

141

142

143

144

145

146

147

148

149

150

151

152

153

Most N₂O production in soil is driven by microorganisms (Braker and Conrad, 2011; Butterbach-Bahl et al., 2013; Syakila and Kroeze, 2011); and the overall microbial activity is markedly higher in the rhizosphere and detritusphere as compared to bulk soil, that is, the soil not directly affected by roots or detritus (Marschner et al., 2012). In intact soil with *in-situ* grown roots, identification of areas directly associated with rhizosphere or detritusphere and quantification of microbial activity dynamics within them are challenging. 2D zymography is a non-destructive technique used for measuring extracellular enzyme activity (Wallenstein and Burns, 2011), which enables the exploration of microbial hotspots at fine spatial scales with high resolutions (Heitkötter and Marschner, 2018; Spohn and Kuzyakov, 2014). Spatial and temporal dynamics of hydrolytic extracellular enzymes, e.g., N-acetylglucosaminidase, have been investigated in root systems and the rhizosphere of various plant species using zymography (Razavi et al., 2016; Sanaullah et al., 2016; Spohn and Kuzyakov, 2013; Spohn and Kuzyakov, 2014; Ma et al., 2017). N-acetylglucosaminidase (a.k.a., chitinase) is involved in both C and N cycling (Tabatabai et al., 2010). Its activity reflects the supply of decomposed organic substances required for N₂O production and thus, is potentially associated with N₂O emission. In zymography, visualization of chitinase activity is achieved by incubating a membrane saturated with a chitinase-specific fluorogenic substrate on the soil surface (Guber et al., 2019). Then, the chitinase activity can be quantified using the fluorescence intensity of the product in the

membrane. The approach can visualize microscale patterns in soil C and N processing and locate hotspots of microbial activity and subsequent N₂O production.

154

155

156

157

158

159

160

161

162

163

164

165

166

167

168

169

170

171

172

173

174

175

176

The N₂O production from decomposing organic sources is closely related to the rate of decomposition; and the dynamics of decomposed C and N are closely coupled affecting associated soil-atmosphere exchange processes (Xia et al., 2018). C and N within plant residue fragments and in their immediate vicinity (Gaillard et al., 1999; Nicolardot et al., 2007; Vedere et al., 2020) can be directly used by microbes that produce N₂O, turning residue fragments into hotspots of microbial activity and N₂O production. Besides decomposed residues, microbial organisms use C and N derived from native soil organic matter (SOM). This can cause a priming effect, that is short-term changes in SOM turnover, triggered by new organic substance inputs (Kuzyakov, 2010; 2000). Previously, priming has been measured in terms of C, defined as accelerated (positive priming) or decelerated (negative priming) emissions of CO₂ derived from SOM. Recently, N₂O priming, that is altered emissions of soil-derived N₂O in response to additions of organic substances, has been suggested as an important contributor to soil N₂O emission (Daly and Hernandez-Ramirez, 2020; Roman-Perez and Hernandez-Ramirez, 2020; Schleusner et al., 2018; Thilakarathna and Hernandez-Ramirez, 2021a; Thilakarathna and Hernandez-Ramirez, 2021b). Simultaneous assessments of CO₂ and N₂O priming in root detritusphere and their dependency on soil pore and moisture conditions can help to better understand changes in SOM stocks and subsequent greenhouse gas emission triggered by plant residues.

The goal of this study was to assess the role of decaying plant roots in N₂O production and emission from soils with contrasting pore architectures under contrasting soil moistures. The use of rhizoboxes, i.e., soil-filled flat rectangular boxes where roots preferentially grow along the

transparent front panel (Mašková and Klimeš, 2020), enabled accounting for the rhizosphere legacy's contribution to N₂O production and emission. Dual-isotope labeling (¹³C and ¹⁵N) allowed for simultaneous tracking of plant originated C and N in mineral, organic, and microbial biomass forms in the soil. Zymograhic measurements of chitinase activity on the intact surfaces of the rhizoboxes provided microscale maps indicative of microbial activity on the decomposing roots and surrounding soil.

The objectives of the study were (i) to assess N₂O and CO₂ emissions from soils with contrasting pore architecture and moisture, containing decomposing *in-situ* grown plant roots, (ii) to quantify the chitinase activity in the root detritusphere and in the bulk soil and to examine associations between its spatio-temporal dynamic and N₂O emissions, (iii) to investigate temporal changes in contributions of root- and soil-derived C and N to emitted N₂O and CO₂ and to microbial biomass during decomposition, and (iv) to test the effects of soil physical conditions (i.e., pore architecture and moisture) on N₂O emission vs. enzyme activity associations in root-based detritusphere.

2. Materials and Methods

2.1 Rhizobox preparation

Soil for the experiment was collected from monoculture switchgrass plots at the Biofuel Cropping System Experiment (BCSE) of the Long-Term Ecological Research site at W. K. Kellogg Biological Station, Michigan, USA. The soil is Kalamazoo loam (fine-loamy, mixed, mesic, Typic Hapludalf), developed on glacial outwash. Monoculture switchgrass has been

grown at BCSE site since 2008. Composite soil samples for the study were collected from 5-10 cm depth and air-dried.

Two materials with contrasting pore-size distributions were prepared for the study from the collected soil: a material with prevalence of >30 μm Ø pores and a material with prevalence of <10 μm Ø pores, referred to further as large-pore and small-pore dominated soils, respectively. Our past work demonstrated the importance of >30 μm Ø pores for decomposition of soil-incorporated plant residues (Negassa et al., 2015). Much faster decomposition and greater CO₂ emissions were observed in the soil materials with sizeable presence of such pores, the differences associated with greater microbial turnover and activity associated with pores of this size range (Kravchenko et al., 2021).

The large-pore soil consisted of the sieved 1-2 mm soil fraction which was obtained by sieving air-dry soil through 1 mm and 2 mm mesh. Small-pore soil was prepared as follows: the 1-2 mm soil fraction was subjected to a series of gentle grindings using mortar and pestle, followed by sieving through a 0.053 mm sieve. The remaining small mineral particles were completely ground using a shatter box until they pass through the 0.053 mm sieve. This approach generated the soils with contrasting pore-size distributions, yet with the comparable mineralogy and microbial structure (Kim et al., 2020; Toosi et al., 2017). Previously conducted X-ray computed micro-tomography scanning of these materials at 2 μ m resolution demonstrated that the large-pore and small-pore soils obtained using this procedure were dominated by >30 μ m Ø and <10 μ m Ø pores, respectively (Toosi et al., 2017).

Since the goal of the study was to explore the contribution of decomposing roots to N_2O emission, it was imperative to ensure that the N_2O originated from root residues could be tracked and distinguished from that originated from SOM. That was achieved by labeling the plants with

¹⁵N via direct N supply to the roots, as opposed to adding ¹⁵N compounds to the soil. This approach required specially constructed rhizoboxes. Rhizoboxes used in this study were transparent plastic containers with dimensions of 4.7 cm x 2 cm x 5.3 cm. Each rhizobox had 8 small holes at the bottom to enable roots to grow out of the soil and into the ¹⁵N labeling solution below (Fig. 1). Each rhizobox also had a removable front panel for zymography measurements (described in *2.5 Zymography analysis*). Rhizoboxes were covered with a UV-light screening tape prior to planting to protect the belowground biomass from other photoautotrophs. A total of 66 rhizoboxes were built - 33 of them were filled with the large-pore soil and the other 33 with the small-pore soil. Approximately 44 g of soil were packed within each rhizobox to achieve a bulk density of 1.15-1.17 g·cm⁻³. Later, 30 rhizoboxes for each soil material were planted with switchgrass, and the remaining 6 boxes were kept as unplanted controls during the entire growing period.

To enhance germination, switchgrass (var. Cave-In-Rock) seeds were stratified by shaking in 8M sulfuric acid for 5 minutes, followed by rinsing 3 times with distilled water. Residual water from the seeds was removed using paper tissues, and the seeds were spread in an even layer on Whatman #1 filter paper inside a petri dish. Another filter paper was placed on the top, and 5 mL of sterile 0.2% potassium nitrate solution was added. The entire petri dish was sealed with parafilm, covered with a paper bag, and placed at 4 °C in a refrigerator. Seeds that germinated within 3 - 5 days were used for the experiment.

One switchgrass seed was placed in each rhizobox, such that half of the seed was buried into the soil. Planted rhizoboxes were placed on a rack tilted at 50° to induce root growth on the removable front panel for future zymography measurements (Fig. 1a). Soil moisture was adjusted to ~60% WFPS at planting and maintained at the same level over the growing period.

To maintain the constant soil moisture, we placed wet cloths at the bottom of rhizobox racks and kept them completely wet during the entire growing period by watering on a daily to twice a day basis. Watering the rhizoboxes from the bottom via wet cloths induced the roots to grow out of the box and into the ¹⁵N labeling solution (Fig. 1b). Switchgrass was grown for 8 weeks in the greenhouse at 24 °C and 16 h of daylight and then subjected to dual labeling (described in 2.2 ¹³C and ¹⁵N plant labeling). Over 8 weeks of growth, the switchgrass seedlings developed firm stalks reaching 11 – 30 cm in height; and had several roots coming out of the holes at the bottom of the rhizoboxes. Unplanted control boxes were placed in the same moisture, temperature, and light settings.

2.2 ¹³C and ¹⁵N plant labeling

After the 8 weeks of growth, the switchgrass was subjected to ¹³C and ¹⁵N labeling. For ¹³C labeling, three ¹³CO₂ pulses were administered with a 5-day interval in-between. For each pulse, 15~20 switchgrass-grown rhizoboxes were placed in a plastic chamber (76 L) along with a beaker with 110 mg of NaH¹³CO₃ (> 99.9% ¹³C). The chamber was sealed with air-impermeable silicon, and 10 mL of 1 M H₂SO₄ was injected into the beaker to complete the acid-carbonate reaction and generate ¹³CO₂ (Fig. 1d). The amount of NaH¹³CO₃ used in the study was chosen to achieve ~40 atom% of ¹³CO₂ in the labeling chamber headspace, which was higher than 33 atom% suggested in Bromand et al. (2001).

For 15 N labeling, we used 50% Hoagland solution (diluted with distilled water, \sim 100 mg N·L-1) containing N as 15 NH₄¹⁵NO₃ (98 atom %, Sigma-Aldrich, MO, USA). Each rhizobox was placed on top of a 50 mL glass beaker filled with the labeling solution in such a way that the

roots, emerging through the holes at the bottom of the rhizobox, were inserted into the liquid inside the beaker (Fig. 1b and c). The volume of the solution in the beaker was ~50 mL; the solution level was checked and refilled every day. An air gap of > 5 mm was always maintained between the liquid and the rhizobox, thus the solution from the beaker did not come into direct contact with the rhizobox's soil. Therefore, the only means by which the switchgrass plants could have received ¹⁵N was through the root uptake from the solution. This design allowed us to ensure that the only source of ¹⁵N within the rhizoboxes was the ¹⁵N from the plant roots. The rhizoboxes were kept on the beakers with the labeling solution for 2 weeks. After 2 weeks of labeling, i.e., a total of 10 weeks of switchgrass growth, the plants were terminated by cutting aboveground biomass. The rhizoboxes were air-dried at room temperature within a ventilation hood for 3 days to readjust the moisture level prior to incubation.

2.3 Incubation experiment and N₂O, N₂, and CO₂ analyses

The 60 root-containing rhizoboxes (plant-terminated, air-dried, see section 2.2) prepared as described in previous sections were separated into 4 experimental batches (Fig. S1). Batch 0 consisted of 3 replicated rhizoboxes of the large-pore and small-pore soils each (a total of 6 rhizoboxes). Batch 0 rhizoboxes were used to characterize soil C and N contents prior to the start of the incubation. The remaining 54 rhizoboxes were subjected to the incubation under two moisture levels, i.e., 40% WPFS and 70% WFPS. These rhizoboxes were grouped into 3 batches, where each batch consisted of a total of 18 rhizoboxes, 9 from each soil fraction. In each batch, 5 replicated rhizoboxes from each soil were randomly assigned to 40% WFPS and the remaining 4 rhizoboxes were assigned to 70% WFPS. Water needed to reach the designed WFPS was added to each box; and the boxes were kept in 450 mL Mason jars. A small beaker with 10 mL of

distilled water was placed within the jar to maintain a high humidity and reduce moisture losses. Jars were tightly sealed and kept in the dark at 21 °C. The rhizoboxes from Batches 1, 2, and 3 were taken apart and used for plant and soil analyses after 3, 21, and 39 days of incubation, respectively (Fig. S1). During the incubation gas samples were collected on days 1, 3 (Batches 1, 2, and 3), 6, 13, 21 (Batches 2 and 3), and 39 (Batch 3). In addition, on all gas sampling days the rhizoboxes from Batch 3 were subjected to zymography analyses.

The no-plant controls were incubated along with Batch 2 rhizoboxes. For the control samples, prior to incubation the moisture was adjusted to 40%, 55%, and 70% WFPS and the average values of the measurements from the 3 samples was reported. The gas emissions and destructive analysis results were also averaged across the moisture levels.

For gas sampling, approximately 50 mL of headspace gas was pulled out from each jar using a 50 mL Luer-Lock syringe, and injected into 3 separate vials for i) ¹⁵N₂O; ii) ¹³CO₂, ⁵N₂ and ¹⁵N₂; and iii) CO₂ and N₂O concentration analyses, respectively. For ¹⁵N₂O and ¹³CO₂/¹⁵N₂ analysis, the headspace gas was injected into 20 mL glass vials at 1 atm pressure. For concentration analysis, the headspace gas was injected into 5.9 mL storage vials (Labco Ltd, Lampeter, U.K.) at 2 atm pressure. The Mason jars were flushed using ultra-pure gas (79% N₂, 21% O₂, and 0% CO₂/N₂O) after each sampling.

N₂O concentration was analyzed using Gas Chromatograph (Agilent Technologies 7890A, Santa Clara, CA, USA) and CO₂ concentration was analyzed with Licor infrared gas analyzer. Isotopic composition of N₂O was measured in stable isotope facility at Michigan State University on an IsoPrime 100 stable isotope ratio mass spectrometer (IRMS) interfaced to a Tracegas inlet system (Elementar, Mt. Laurel, NJ) (Sutka et al., 2003). Using Helium as the carrier gas, the Tracegas inlet removes CO₂ and water, before cryofocussing N₂O onto a gas

chromatographic column, before introduction to the IRMS. The calibration procedure included analyses of isotopically distinct standards of enriched N_2O ($^{15}N_2O$, > 98 atom%, Cambridge Isotope Laboratories, Inc. Andover, MA, USA). Each day, we analyzed at least four of the calibration standards (range of 3-20 nmole N_2O). Samples of CO_2 were measured using the same procedure, except the Tracegas system was set so as not to remove CO_2 from the sample. The standards were prepared by mixing our laboratory standard gas with different amounts of enriched CO_2 ($^{13}CO_2$, 99 atom %, Sigma-Aldrich, MO, USA) ranged 9-65 nmole CO_2 . Concentration of N_2 in gas samples was analyzed using a gas chromatograph (Hewlett Packard 5890) with a modified inlet interfaced to an Isoprime IRMS (Elementar) (Roberts et al., 2000). The N_2 air of 3-30 µmole range was used for calibration. Minimum detection limit of Isoprime100 is \sim 1.5 nmole N_2O , \sim 1.5 nmole CO_2 , and \sim 1 µmole N_2 .

2.4 Zymography analysis

A hydrophilic polyamide membrane filter (Tao Yuan, China) 4 cm x 5 cm in size was used for zymography measurements. We used 6 mM 4-Methylumbelliferyl N-acetyl-glucosaminide (MUF-NAG; Sigma-Aldrich, MO, USA) solution as a substrate for chitinase (Spohn and Kuzyakov, 2014). Upon contact with chitinase, the substrate releases florescent product (4-methylumbelliferone) that can be detected under ultraviolet light (Guber et al., 2018). We used Canon EOS Rebel T6 camera with a Canon 75-300 mm f/4-5.6 III Telephoto Zoom Lens to take zymograms (Guber et al., 2021). Batch 3 rhizoboxes were repeatedly measured on days 1, 3, 6, 13, and 21 after the gas collection. The soil surface for zymography of each rhizobox was sprayed with distilled water to ensure hydraulic contact between the soil surface

and the membrane. The amount of sprayed water was < 120 mg, thus could only have negligible, if any, effect on the soil moisture level of the entire rhizobox (for comparison, the amount of water within a rhizobox at 40%WFPS was equal to ~9 g). Then the membrane was soaked with MUF-NAG, attached to the soil surface and fixed with a holding frame. The sample was placed in the dark hood with the camera installed at the top and with ultraviolet light source. The membrane was photographed every minute for a total of 50 minutes per sample.

334

335

336

337

338

339

340

341

342

343

344

345

346

347

348

349

350

351

352

353

354

355

356

The zymograms were calibrated and converted into maps of enzyme activity using MATLAB 9.5 (MathWorks, MA, USA). A calibration was performed by adopting the method developed by Guber et al. (2019). We calculated root and soil enzyme activity by separating the decomposing root and soil areas on each zymogram. For that, a picture of the soil surface, i.e., a reference image, was taken prior to zymography (Fig. S2a). Then a series of image processing steps – background removal, automatic adjustment of brightness and contrast, Gaussian blur (pixel 2.0), and auto local thresholding (default option) in Fiji (Schindelin et al., 2012) – was applied to the reference images (Fig. S2). The resultant binary image was then subjected to particle analyzer imbedded in BoneJ plugin (Doube et al., 2010) to exclusively select root particles. The final reference image provided information on the location of the roots on the rhizobox surfaces (Fig. S2f and Fig 2c). The areas of the decomposing root and the soil were then multiplied by the average enzyme activity values calculated from the zymograms to obtain separated enzyme activity values for the decomposing roots and for the soil (Fig. 2d and e). It should be noted that recent efforts in *in-situ* rhizosphere mapping using zymography tools demonstrated that the spatial extent of microbial hotspots around roots does not exceed 50-250 um (Khosrozadeh et al., 2021 in review). In the current study, a portion of these very narrow active layers of soil surrounding decomposing roots was likely classified as root surfaces. Thus,

what we report as chitinase activity on the decomposing roots likely includes a portion of the detritusphere that was former rhizosphere in immediate proximity (<500 µm) to the roots.

Chitinase activity during root decomposition was analyzed and reported as i) total chitinase activity (Fig. 2b), which is the mean chitinase activity on the entire zymography surface, ii) root chitinase activity, which is the mean chitinase activity on the decomposing root surfaces only (Fig. 2d), and iii) soil chitinase activity, which is the mean chitinase activity on the soil surface (i.e., bulk soil) (Fig. 2e). That is, mean chitinase activity in the area of interest (presented as brown color in Fig. 2d and e) was used for decomposing root and soil chitinase activities. Note that, while for brevity in the rest of the text we use term "root chitinase activity", it refers not to the activity on the living roots but to the activity on the surfaces of decomposing roots.

2.5 Plant and soil analysis

Rhizoboxes of Batches 1, 2, and 3 were subjected to destructive analysis on days 3, 21, and 39 of incubation, respectively. Roots and soil in the rhizoboxes were separated by using forceps. For dissolved organic C (DOC), total dissolved nitrogen (TDN), microbial biomass, ammonium (NH₄⁺) and nitrate (NO₃⁻), 10 g of fresh, wet soil was weighed immediately after collection and added to a vial with 50 mL of 2 M KCl solution (1:5 soil: solution ratio). The resultant soil suspension was homogenized using an orbital shaker set to 180 rpm for 24 h and centrifuged with 5000 rpm for 10 min. The supernatant was filtered through a 0.45 µm membrane. Total (i.e., not isotope-specific) DOC and TDN were analyzed using Shimadzu TOC-Vcph C analyzer with a total nitrogen module (Shimadzu, Tokyo, Japan). Inorganic N (NH₄⁺ and

NO₃-) were determined spectrophotometrically at 630 and 530 nm, using salicylate-cyanurate method (Sinsabaugh et al., 2000) and vanadium method (Doane and Horwáth, 2003), respectively. Dissolved organic N (DON) was calculated by subtracting inorganic N from TDN. Microbial biomass was measured using a modified version of the fumigation-extraction method (Vance et al., 1987). Fumigated and non-fumigated KCl (2M) soil extracts were analyzed using Shimadzu TOC-Vcph C analyzer, and the difference between fumigated and non-fumigated samples was divided by K_{ec} (0.45) and K_{en} (0.54) to obtain microbial biomass C and N, respectively (Brookes et al., 1985; Vance et al., 1987). However, most estimates of microbial biomass N had considerable uncertainty due to instrument failure, thus only microbial biomass C (MBC) was reported.

Remaining soil and roots were air-dried for 2 days and homogenized to measure total C and N contents using Costech elemental combustion system (Costech Analytical Technologies Inc., CA, USA). Additionally, in the rhizoboxes from batch 3 we also collected and analyzed total C and N of soil particles directly attached to the roots, i.e., rhizosphere soil, separately. Measurements of δ^{13} C and δ^{15} N in solid samples, i.e., soil and plant tissues, were performed in stable isotope facility at Michigan State University using an Isoprime Vision IRMS interfaced to a Vario Isotope Cube elemental analyzer (Elementar). Isotopic values of KCl extracts were determined by freeze-drying the solution and analyzing the isotopic values of the power using EA-IRMS in Environmental Molecular Sciences Laboratory (EMSL) at Pacific Northwest National Laboratory.

Relative differences in isotopic composition to the standards (δ) were converted to atom% to calculate switchgrass root-derived C and N in all pools (gas, microbial biomass, dissolved organic C, and total dissolved N).

401

402

403

409

410

411

412

404 Atom% = {
$$[(\delta \cdot 1000^{-1} + 1) \cdot R_R]^{-1} + 1$$
}⁻¹ · 100 Eq. 1

where δ (‰) is relative difference in isotope ratios and R_R is the ratio of the heavy isotopes to the light isotopes (13 C/ 12 C and 14 N/ 15 N). The fraction from the labeled residue (f_{res}) in certain pool is calculated as:

408
$$f_{\text{res}} = (\text{Atom}\%_{\text{otrt}} - \text{Atom}\%_{\text{control}}) \cdot (\text{Atom}\%_{\text{root}} - \text{Atom}\%_{\text{control}})$$
Eq. 2

where Atom%trt is atom% (atom%¹³C or ¹⁵N) of the treatments in the certain pool, Atom%control is the atom% of unamended sample of corresponding pools (¹³C or ¹⁵N natural abundance), and Atom%root is the atom% of the original labeled roots. Then the mass or concentration of the pool derived from the labeled residue (Cres) was calculated as:

$$C_{res} = C_{total} * f_{res}$$
 Eq. 3

Where C_{total} is the total mass or concentration of the pool. The pool derived from soil (C_{soil}) was calculated as:

$$C_{\text{soil}} = C_{\text{total}} * (1 - f_{\text{res}})$$
 Eq. 4

Delta (δ) value of microbial biomass (δ_{MB}) was calculated from the δ values of fumigated and non-fumigated extracts as:

$$\delta_{MB} = [\delta_F \cdot C_F - \delta_{NF} \cdot C_{NF}] \cdot C_{MB}^{-1}$$

Where δ_F and δ_{NF} are δ_{NF} are δ_{NF} are concentrations (C or N) of fumigated and non-fumigated samples; and δ_{NF} are between δ_{NF} and δ_{NF} are concentrations (C or N) of fumigated and non-fumigated samples; and δ_{NF} are between δ_{NF} and δ_{NF} .

The rates of CO₂ and N₂O priming of decomposing roots were calculated by subtracting the average CO₂ and N₂O emission rate from unplanted control soils from each observation of soil-derived CO₂ and N₂O emissions of the treatments. Cumulative CO₂ and N₂O priming effects, which are defined as the differences in cumulative soil-derived N₂O and CO₂ emissions between treatments and no-plant controls, were calculated as the sum of the product of the priming rates and the time intervals from day 1 to day 21. Cumulative priming was determined by each rhizobox, thus the rhizoboxes belonged to batch 1 (took apart for destructive analysis on day 3) were not included for calculation.

2.7 Statistical analysis

Data were analyzed using a mixed-model approach implemented in PROC MIXED procedure of SAS 9.4 (SAS Institute Inc., NC, USA). For gas flux data, including total, root-derived, soil-derived and fractions of CO₂·N₂O, total N₂, and rates of CO₂·N₂O priming; and for zymography data, including total, root, and soil chitinase activity, the statistical model consisted of fixed effects of soil (large- vs. small-pore dominated soils), soil moisture (40 vs. 70 %WFPS), time, and their interactions. The statistical model also included the random effect of individual rhizoboxes nested within materials and moistures. Time was treated as a repeated measure factor, with individual rhizoboxes used as a subject of repeated measurements. The repeated measures analysis was conducted using the approach outlined in Milliken and Johnson (2002).

For cumulative gas emissions, including cumulative CO₂ and N₂O, and cumulative priming effects, and for total C and N derived from roots the statistical model consisted of fixed effects of material, moisture, and their interactions. For measurements from destructive analysis, including total C, total organic N, MBC, and inorganic N, the statistical model consisted of fixed effects of material, moisture, time, and their interactions.

The relationships between pairs of continuous variables (e.g., between CO₂ and N₂O or between chitinase activity and emitted gases) were explored by fitting statistical models that included the mentioned above categorical factors, the linear effects of the studied continuous variable, and the interactions between them. The latter enabled assessing the differences in the relationships between the continuous variables at different levels of the soil pore or soil moisture effects. When the regression slopes were not significantly different between the soil pore sizes (p>0.05), results of fitting a model with a common regression slope were reported.

For all datasets, the normality assumption was evaluated by checking normal probability plots, and when violated, the data were natural log-transformed (Milliken and Johnson, 2009). The homogeneity of variances assumption was tested by Levene's test based on the absolute values of model residuals. When the homogeneity of variances assumption was found violated, the analysis with heterogeneous variances was conducted (Milliken and Johnson, 2002). Statistical significances were indicated as *** (p< 0.01) and ** (p< 0.05), with tendency as * (p< 0.10).

3. Results

3.1 Switchgrass growth and its effects on soil characteristics

At plant termination after 10 weeks of growth, the root biomass (av. 426 mg per rhizobox) and the aboveground biomass (av. 130 mg per rhizobox) in the two studied soils, i.e., the large- and small-pore soils, were similar (p> 0.10, data not shown). Total C, N, atom%¹³C, and atom%¹⁵N of the roots also did not differ between the soils (p> 0.10, Table 1). The area occupied by the roots on the side of the rhizobox subjected to zymography constituted on average 7.5% of the soil surface and were similar in the large- and small-pore soils (p> 0.10, data not shown). Immediately after plant termination, the two soils did not differ in terms of total C and organic N, inorganic N, and isotopic signatures of C and N (p> 0.10) (Table 1). The large-pore soil had lower MBC (384 mg C kg⁻¹ soil) than the small-pore soil (571 mg C kg⁻¹ soil) (p< 0.05, Table 1).

$3.2 N_2O$, CO_2 , and N_2 emissions

Total, root-derived, and soil-derived N₂O emissions were greater in the large-pore soil compared to the small-pore soil, and greater at 70% WFPS compared to 40% WFPS throughout the incubation (Fig. 3a and b, Table S1). Soil pore size strongly regulated total N₂O emissions (*p*< 0.01). After 21 days of incubation the large-pore soil had 11 and 28 times higher cumulative total N₂O emissions than small-pore soil at 40% and 70% WFPS, respectively (Fig. 4a and b). Contrarily, N₂O emission from the unplanted control rhizoboxes was not statistically different in the two soil materials. Soil with moisture of 70% WFPS had 3.5 and 1.4 times higher total N₂O emissions compared to that with 40% WFPS in the large- and small-pore soils, respectively.

The fraction of N_2O derived from decomposing roots also differed between the two soils. While in the large-pore soil the root-derived N_2O accounted for > 60% of the total emitted N_2O

for 3-21 days of incubation, in the small-pore soil it peaked at 60% on day 3 and continuously decreased to < 40% on day 21 (Fig. 3c). Although the higher moisture level increased the total amount of emitted root-derived N_2O , it did not affect the fraction of the emitted N_2O that was derived from the root residues.

In contrast to N₂O emissions, CO₂ emissions were weakly controlled by pore sizes and not regulated by moisture levels (Fig. S3). In all treatments, the maximum CO₂ emission rate was reached on days 3~6 and then decreased dramatically. The large-pore soil tended to have greater CO₂ emissions compared to the small-pore soil (p< 0.10) but only at a later stage of the incubation (Fig. S3a). Unlike N₂O, CO₂ emissions were not affected by soil moisture (p> 0.10). Cumulative CO₂ emissions from planted rhizoboxes were ~2 times greater than that from unplanted control soils (Fig. 4c and d).

Cumulative N₂O priming was governed only by pore sizes (p< 0.01, marked as red arrows in Fig. 4a and b). However, the rate of N₂O priming over 21 days was influenced by both pore size (p< 0.01) and moisture level (p< 0.05), and the moisture effect was more noticeable in the large-pore soils (Fig. 5). The cumulative N₂O priming was positive in all treatments except for the small pore soils at 40% WFPS, and 20~25 times greater in the large- than in the small pore soils (Fig. 4a and b). Cumulative CO₂ priming (marked as red arrows in Fig. 4c and d) tended to differ between pore sizes (p< 0.10) and moisture levels (p< 0.10). The mean of cumulative CO₂ priming at 40% WFPS was negative, but only the large-pore soils at 40% WFPS had the statistical difference from 0. At 70% WFPS, cumulative CO₂ priming in both pore treatments were not significantly different from 0 (Fig 4c and d).

CO₂ emissions were positively correlated with N₂O emissions, however, the strength of the correlation depended on the soil. Only 7% of variation in N₂O emissions was explained by

the variation in CO₂ emissions in the large-pore soil, while 68% of the variation in N₂O emissions was explained by the variation in CO₂ emissions in small-pore soil (Fig. 6). In small-pore soil, N₂ emissions from root-containing rhizoboxes were not significantly different from the unplanted control rhizoboxes. The difference in N₂ emissions between planted and unplanted soils was greater than 0 on day 6 in the large-pore soil (Fig. 7).

3.3 Chitinase activity dynamics during root decomposition

Chitinase activities on root surfaces and in bulk soil were consistently higher in the large-pore soil compared to the small-pore soil, and at 70% WFPS compared to 40% WFPS (p< 0.05, Fig. 8). Chitinase activity on the decomposing roots was significantly higher than chitinase activity in the bulk soil regardless of the soil pore size and moisture level (*p*< 0.01, Table S2). While root chitinase activity increased drastically and reached a maximum on day 3-6 (Fig. 8b and e), the chitinase activity in the bulk soil was the highest during 6-13 days of the incubation (Fig. 8c and f). At 40% WFPS, the large- and small-pore soils had maximum root enzyme activity of 1.2 and 0.4 pmol·min⁻¹·cm⁻², respectively. At 70% WFPS, the activity was higher than at 40% WFPS, with 2.4 pmol·min⁻¹·cm⁻² in the large-pore and 1.1 pmol·min⁻¹·cm⁻² in the small-pore soil.

Both root-derived N_2O and CO_2 emission rates were positively correlated with root chitinase activity (Fig. S4a and b). While the root chitinase activity explained 22% of the variability in the root-derived N_2O emission rate (p< 0.01), it explained only 3% of the variability in the root-derived CO_2 emissions (p< 0.05). Neither soil-derived N_2O nor CO_2

emission correlated with soil chitinase activity (Fig. S4c and d). The regression slopes were not significantly different between the soil pore sizes and moisture levels.

3.4 Soil inorganic N, plant-derived C and N, and microbial biomass C

Although there were no differences in NH₄⁺ and NO₃⁻ contents between the large- and small-pore soils after plant termination before incubation, the large-pore soil tended to have higher inorganic N content once the root decomposition started. In the large-pore soil, NH₄⁺ was significantly higher than that in the small-pore soil on day 3 (10.6 vs. 5.9 mg N·kg⁻¹ soil) and on day 39 (1.7 vs. 1.1 mg N·kg⁻¹ soil) (Fig. S5a). Likewise, NO₃⁻ was significantly higher in the large- compared to small-pore soil on day 21 (2.2 vs. 1.3 mg N·kg⁻¹ soil) (Fig. S5b). Ammonium rapidly increased at the early stage of the root decomposition (~ day 3) and decreased afterward. Nitrate increased continuously throughout the decomposition, reaching 20.4 mg N·kg⁻¹ soil on day 39. No effect of moisture level was detected on NH₄⁺ or NO₃⁻ contents.

While there were no differences in DOC between the two soils on day 0, the effect of pore size on DOC content developed as the incubation proceeded (Fig. S6a). The difference in DOC between the pore sizes was the greatest on day 39, equal to 98 and 52 mg $C \cdot kg^{-1}$ soil for the large- and small-pore soils, respectively. Moisture level did not affect the DOC. DON increased quickly and reached 74 and 60 mg $N \cdot kg^{-1}$ soil within 3 days for the large- and small-pore soils, respectively (Fig. S6b). It further increased until day 21 and decreased back to the same level that was observed on day 3, which was still higher than the initial level. Consistent with DOC, the DON was not affected by moisture level, but was greater in the large- than in small-pore soils (p< 0.01). MBC on day 39 was 100-140 mg $C \cdot kg^{-1}$, and 25 and 15% of it was derived from the

root C in the large- and small-pore soils, respectively (Fig. S7). While total MBC was not affected by the pore size and moisture level, the root-derived MBC was higher in the large- than in small-pore soils at the end of the incubation (day 39) (p< 0.05).

At the end of the incubation the former rhizosphere soil, that is, the soil particles directly attached to the decomposing roots, had higher C and N contents, as well as their fractions derived from the roots, than the bulk soil (p< 0.01, Fig. S8). Total soil C and N contents were greater in the large- compared to small-pore soils, but the fractions of C and N originated from the roots were not affected by pore sizes. Moisture level did not affect total soil C and N in the former rhizosphere soil, nor the fraction of C and N originated from decomposing roots (Fig. S8c and d).

4. Discussion

4.1. In-situ grown roots in root decomposition studies

The current shortage of decomposition studies that use *in-situ* grown roots is likely driven by several experimental limitations: 1) changes of the root mass during decomposition are not trackable, since it is not possible to measure the initial mass of the *in-situ* roots; 2) locations of the root residues during decomposition are not known, leading to difficulties in locating hotspots of microbial activity and N₂O production; and 3) tracking the fate of root-originated N, for example with a commonly used approach of ¹⁵N stable isotope labeling, can be a challenge because of difficulties in achieving a sufficiently high level of label just within the roots without contaminating the soil. Kim et al. (2020) overcame the first two limitations by employing X-ray computed microtomography before and after incubating the experimental microcosms, which

allowed measurements of initial root volumes, determination of root volume losses during decomposition, and visualization of root positions within the samples. The current study overcame the third limitation by employing an innovative system of supplying plant roots with N without soil contamination and ensuring that roots are the only source of ¹⁵N in the soil.

4.2. Soil pore size as a key driver of N_2O emissions

Consistent with expectations and previous studies (Schaufler et al., 2010; Shelton et al., 2000), during *in-situ* root decomposition, greater total N₂O emissions and both greater root- and soil-derived N₂O were observed at 70% WFPS than at 40% WFPS settings (Fig. 3, 4, and Table S1). High soil moisture content leads to lower O₂ availability and faster NO₃⁻¹ diffusion, promoting N₂O production via denitrification (Bollmann and Conrad, 1998; Butterbach-Bahl et al., 2013; Chen et al., 2013; Myrold and Tiedje, 1985). However, our results suggest that prevailing soil pore architecture can play a much more important role in stimulating N₂O production and transport to the soil surface than soil moisture content (Fig. 9). The cumulative amount of N₂O emitted from the large-pore soil was ~21 times greater than that emitted from the small-pore soil, while the cumulative amount emitted at 70% WFPS, i.e., the WFPS of commonly observed maximal N₂O emissions (Davidson, 1991; Schmidt et al., 2000) – was only 3.5 times greater than that at 40% WFPS. That is, in the studied soil materials with contrasting pore architectures, the effect of soil pore architecture was more than 6 times greater than the effect of soil moisture.

At first glance, greater emissions of N₂O from soils dominated by $>30 \mu m \ \emptyset$ (large) pores than from soils dominated by $<10 \mu m \ \emptyset$ (small) pores seem paradoxical. If the overall

anaerobicity were the controlling factor of N₂O production, soils dominated by small pores, with their high pore tortuosity which reduces gas diffusion and thus leads to O2 shortages, would produce more N₂O (Groffman and Tiedje, 1989; Zaman et al., 2012). Yet, higher N₂O emissions from the large- than from small-pore soils have been reported before (Gu et al., 2013; Kaiser and Heinemeyer, 1996; Kravchenko et al., 2017; Weitz et al., 2001). It has been proposed that the reason for lower N₂O emissions is a greater extent of complete denitrification to N₂ in the smallpore dominated soils, driven by their low O₂ levels and slow rates of gas diffusion preventing an escape of produced N₂O (Gu et al., 2013; Kaiser and Heinemeyer, 1996; Kravchenko et al., 2017; Weitz et al., 2001). N₂O is highly water soluble and spatial heterogeneity in distribution patterns of soil water can markedly decrease its diffusion in gaseous phase (Shcherbak and Robertson, 2019), further benefiting the complete denitrification. Surprisingly, our findings challenge this explanation. The total N₂ emission from the small-pore soil with decomposing plant roots did not exceed that of the unplanted control soil (Fig. 7b). On the contrary, in the large-pore soil, a significant increase in N₂ emission relative to the control was observed after 6 days of root decomposition (Fig. 7a); an increase that was concurrent with high N₂O emissions (Fig. 3). These results suggest that greater N₂O to N₂ reduction in soils dominated by small pores can only be a minor contributor to their ~21-fold lower N₂O emissions.

597

598

599

600

601

602

603

604

605

606

607

608

609

610

611

612

613

614

615

616

617

618

619

The alternative explanation we propose is that greater water absorption by tissues of plant residues (Iqbal et al., 2013; Myrold et al., 1981; Quemada and Cabrera, 2002) in the large-pore dominated soil creates microenvironmental conditions favorable to denitrification, leading to enhanced production of both N₂O and N₂. Decomposing plant residues absorb water from adjacent soil pores, creating local micro-gradients of moisture within surrounding soil (~150 μm from the plant residues) (Kim et al., 2020; Kutlu et al., 2018). This "sponge effect" (Kravchenko

et al., 2017; Kim et al., 2020) is more pronounced when the soil around the residue is dominated by large rather than small pores, due to lower water retention by soil with larger pores. Such local anoxic conditions within the decomposing roots themselves and in the adjacent former rhizosphere soil were accompanied by high available organic content (Fig S5 and S6) and active microbial communities, serving as respective sources and drivers of N₂O production (Fig. 9). At the same time, some large pores outside the zone influenced by the sponge effect are atmosphere-connected, thus instrumental to the eventual emission of produced N₂O and N₂ (Kim et al., 2020). Consistent with this explanation, in the large-pore soil, > 60% of emitted N₂O was root-derived for the entire incubation duration, while roots' contribution was much lower in the small-pore soil (Fig. 3c). Our findings emphasize the importance of root residues in soils dominated by large (>30 µm) pores with respect to increased N₂O emissions and elucidate a potential mechanism behind such increases (Fig. 9). Specifically, root residues act as powerful hotspots of N₂O production, while diffusion of produced N₂O via large pores magnifies the quantities emitted.

Soil pore architecture is known to markedly affect C processing in the presence of plentiful and/or newly added C inputs (Bouckaert et al., 2013; Hailing et al., 2013; Juarez et al., 2013; Salome et al., 2010), however the pore effect is often reported as negligible when such inputs are absent (Kravchenko and Guber, 2017; Negassa et al., 2015). Pore architecture influence on N processing seems to be similarly driven by the abundance of organics. For example, previous studies that investigated the interactive role of soil pores and moisture content on N₂O emissions, without new C additions and/or inherent large sources of organics, found only a marginal pore effect on soil-derived N₂O (Mangalassery et al., 2013; Rohe et al., 2021). Yet, in

our study, with its large root biomass available for decomposition, pore architecture had a major influence on both root- and soil-derived N₂O production and emission.

In this study we worked with the soil materials built to maximize the contrasts in pore architecture characteristics. While it is a feasible approach for elucidating the role of pores as drivers of soil processes, such contrasting conditions are rare in intact field soils with their wide range of naturally occurring pore sizes and shapes. Thus, the effect of the pore architecture in the field is probably lower than what we observed in our experiment. Likewise, natural root senescence and decay occur asynchronously in field switchgrass systems, while all roots started to decay simultaneously in this study. Simultaneous decay maximized the roots' contribution to N₂O production here, while a more modest effect might be expected in the field conditions. Our experimental condition of 40% and 70% WFPS soil water content also suggest that it may be applicable particularly in upland soils where the moisture content ranges are similar to our experimental settings.

4.3. Relationships between chitinase activity, root decomposition, and N₂O emissions

Immediately after plant termination, the activity of chitinase was similar between the large- and small-pore soils, either near the roots or in the bulk soil (Fig. 8). However, after the onset of incubation, the chitinase activity in the large-pore soil increased dramatically, in contrast to only a minor increase in small-pore soil. The high activity in the large-pore soil was maintained during 21 days of root decomposition (Fig. 8). Chitinase activity can be viewed as a curser of organic matter decomposition since it is involved in both C and N mineralization and cycling (Sinsabaugh and Moorhead, 1994; Tabatabai et al., 2010). Greater chitinase activity and

consequently, decomposition of organic substances, took place in the large- than in the small-pore soil (Fig. 9).

664

665

666

667

668

669

670

671

672

673

674

675

676

677

678

679

680

681

682

683

684

685

686

Note that switchgrass plants grew within two contrasting soils from their germination and, subsequently, their roots were decomposed *in-situ*. Thus, by the time of plant termination (10 weeks after sowing), the microbial community structure in the two soils might have been already different, because dominant microbial organisms and their activity depend on pore space characteristics (Gupta and Germida, 2015). Fungi are often more abundant in sand and grow better in pores of >10 µm (Chenu and Cosentino, 2011; Kögel-Knabner et al., 2008; Witzgall et al., 2021), while bacteria are often preferentially located in <10 μm pores (Schlüter et al., 2018). Thus, the large-pore soil might have been more favorable to fungal growth, while small-pore soil favored bacterial growth. Since switchgrass roots commonly form symbiotic relationships with arbuscular mycorrhizal fungi (Jach-Smith and Jackson, 2020), we speculate that fungal biomass that accumulated during switchgrass growth played an important role in cycling of root-derived N; and large amounts of labeled ¹³C and ¹⁵N processed by living switchgrass plants might have been assimilated into fungal biomass and hyphae. Higher amounts of chitin-rich fungal necromass and its processing may explain the substantially higher chitinase activity and concomitantly greater N₂O contribution from root-derived N in the large- than in small-pore soils (Fig. 3c).

Microenvironmental conditions after plant termination were also more beneficial for microbial decomposers, especially fungi, in the large- than in small-pore dominated soils (Fig. 9). Adequate supply of O₂ (Keiluweit et al., 2017) and greater organic inputs from roots of growing plants (Quigley et al., 2018) are regarded as the main drivers of enhanced microbial activity and high microbial turnover within large pores (Kravchenko et al., 2021). Specifically,

we surmise that a succession of fungi from mycorrhiza to saprotrophs occurred after plant termination (Herman et al., 2012), resulting in chitinase production and efficient decomposition of chitin-rich necromass from the fungal biomass and hyphae in the former rhizosphere.

Saprotrophs prefer well-aerated large-pore soil and require less N compared to mycorrhiza (Leake et al., 2003), thus excess N from mycorrhizal fungal necromass might have been used for denitrification.

While we did not directly measure fungal activity, it is known that fungi contribute more than bacteria to chitinase production in soil (De Boer et al., 1999; Miller et al., 1998; Yanai and Toyota, 2005), thus we assume that the chitinase activity measured in this study is indicative of fungal activity. We suggest that enhanced fungal activity was responsible for the observed 5-7-fold higher chitinase activity in the bulk soil of the large- than small-pore soils that developed within just the first few days of incubation (Fig. 8c and 8f).

Higher NH_4^+ during the first few days of incubation (Fig. S5a) in the large-pore soil was another indicator of faster decomposition and N mineralization. A positive correlation between the chitinase activity measured directly on the decomposing roots (i.e., root chitinase activity) and the rate of emission of root-derived N_2O ($R^2 = 0.22$) supports the link between decomposition of chitin contained in/around roots and N_2O production (Fig. S4a). We speculate that the rapid decomposition of roots in the large-pore soils contributed to a great supply of inorganic N. Nitrate from decomposed organic substances (e.g., chitin) can be immediately utilized by denitrifying microbes (Fan et al., 2014), adding to the more pronounced root-derived N_2O production in the large-pore soils (Fig. 4).

High N₂O emissions from the large-pore soil were maintained over 21 days of root decomposition and only slightly decreased by day 39. In contrast, in the small-pore soil the N₂O emissions decreased much faster (Fig. 3a and b), accompanied by a decrease in the proportion of root-derived N₂O (Fig. 3c). Apparently, the switchgrass root-based hotspots of N₂O production in the soil dominated by large pores can last longer and contribute substantially to the total emissions for more than a month after plant termination. This finding contradicts our previous results where N₂O reached its base level in 7-14 days after the start of incubation with leaf residues (Kravchenko et al., 2017; 2018) and with switchgrass root residues (Kim et al., 2021). Similarly, short-termed flashes of N₂O emissions were reported in other plant residue decomposition studies, where N₂O emission rates reached base levels within 14-32 days (Begum et al., 2014; Fan et al., 2014; Köbke et al., 2018; Li et al., 2016). It should be noted that in our previous work, as in most other studies, plant residues were incorporated into sieved soil.

We attribute the longevity of N₂O emissions in the current experiment to the rhizosphere legacy, that is, to roots being decomposed *in-situ*. Rhizosphere represents an ideal microenvironment for microorganisms (Chau et al., 2011; Vieira et al., 2020); and in this study for almost 10 weeks the rhizosphere soil continuously received root exudates and other rhizodeposits such as lysates, dead fine roots, and mucilage (Lynch and Whipps, 1990; Nguyen, 2003). Upon plant termination, not only the decaying roots but also the previously deposited organic inputs and the necromass of the organisms assimilating root exudates in the former rhizosphere's soil were the subjects of intense decomposition by abundant microbial communities, especially active in the optimal microenvironment of large pores (Kravchenko et al., 2021). Other root-mediated changes in the rhizosphere (Blossfeld et al., 2013; Hinsinger et

al., 2003) can also change pathways and magnitudes of N₂O production. For instance, decreased pH can stimulate heterotrophic denitrification as the main N₂O production pathway during decomposition (Duan et al., 2019). Our results suggest that micro- and mesocosm experiments that use root residues removed from their original soil locations and mix them with either sieved or even intact soil might substantially underestimate the durations and intensities of N₂O emissions.

4.5. Decoupled N₂O and CO₂ production in large-pore dominated soils

Emission of CO₂ is one of the general indicators of microbial activity, and since many soil processes – including residue decomposition, nitrification, and denitrification – are mediated by soil microbes, in residue amended soils CO₂ and N₂O emissions are often found to be positively correlated (Azam et al., 2002; Millar and Baggs, 2004). Yet, in this study, such correlation was present only in the small-pore (R²=0.68), but not in the large-pore (R²=0.07) soils (Fig. 6). At the same level of CO₂ emission, i.e., same general microbial activity, the large-pore soil emitted 10-20 times more N₂O compared to the small-pore soil (Figs. 4 and 6). This decoupling of CO₂ and N₂O emissions suggests that different groups of microorganisms were involved in N₂O production in the large- and small-pore dominated soil, and the groups active in the large-pore soils were those that produced N₂O but not CO₂. Further experiments accompanied by analyses of microbial community compositions are needed to further explore the observed differences.

4.6. N₂O priming

Roots, *in-situ* decomposing in the large-pore soil, were not only a major source of N₂O; they also stimulated N₂O production from decomposition of intrinsic SOM via positive N₂O priming (Fig. 4a and b, Fig. 9). The phenomenon of positive N₂O priming has been only recently brought to attention of scientific community (Roman-Perez and Hernandez-Ramirez, 2020) and its exact mechanisms are still poorly understood. Roman-Perez and Hernandez-Ramirez (2020) reported that high SOM-C and SOM-N availability generated a positive N₂O priming effects; the authors suggested a successional shift in priming mechanisms from stoichiometry to N-mining. Since the availability of SOM in the rhizosphere can increase due to root exudates during plant growth (Li et al., 2021), the rhizosphere legacy might have maximized the magnitude of N₂O priming.

Our N₂O and CO₂ priming results further support the notion of decoupling of N₂O and CO₂ production in presence of *in-situ* decomposing switchgrass roots, the effect especially pronounced in the large-pore soils, but present in the small-pore soil as well. Positive N₂O priming coincided with negative or negligible CO₂ priming (Fig. 4). Negative C priming is typically observed when the newly added organic inputs are recalcitrant (Guenet et al., 2010; Zhang et al., 2019), but additions of highly labile substrate also were reported to cause preferential substrate utilization leading to negative priming (Kuzyakov and Bol, 2006). Since C:N ratios of the studied young switchgrass roots were relatively low (~15), it is possible that they were the preferred source of C to soil microorganisms over SOM, resulting in reduced SOM decomposition. Yet, some microorganisms, specifically those responsible for N₂O production from both root and soil N sources were apparently strongly stimulated during root decomposition.

Such joint stimulation took place on the root surfaces and in their close proximity, probably in the former rhizosphere, rather than in the bulk soil. Notably, the temporal patterns of N₂O priming (Fig. 5) closely followed those of the chitinase activity on the decomposing roots (Fig. 8b and e), while there were no similarities with the chitinase activity patterns in bulk soil (Fig. 8c and f). Also, soil chitinase activity and soil-derived N₂O emission were not related to each other (Fig. S4c), while the chitinase activity on the root surfaces and the plant-derived N₂O emission were positively correlated (Fig. S4a). Previous reports suggest that the extracellular enzymes produced in response to newly added organic inputs can also be efficient at decomposing inherent SOM and, hence, can promote positive priming (Fontaine et al., 2003; Wu et al., 1993). Thus, the greater extent of N₂O priming in the soil dominated by large pores (Fig. 4a, b, and Fig. 5) is likely driven by higher enzyme activity near decomposing roots there (Fig. 8), which stimulated the decomposition of not only the roots but also of the N-containing SOM, resulting in higher contents of mineral N in the large-pore soil (Fig. S5). Strategical procurement of N but not C from SOM by microorganisms involved in N₂O production apparently can take place in the former rhizosphere soil during root residue decomposition.

791

792

793

794

795

796

797

798

776

777

778

779

780

781

782

783

784

785

786

787

788

789

790

5. Concluding remarks

The effect of soil pore architecture on N_2O production from soil with *in-situ* decomposing switchgrass roots was 6 times higher than that of the soil moisture. Markedly greater quantities of N_2O were emitted from the soil dominated by the large (>30 μ m) pores than from the soil dominated by small (<10 μ m) pores, while only modestly higher emissions were observed in incubations at 70% as compared to 40% WFPS. Longevity of N_2O emission hotspots in the large-pore soils exceeded that of the small-pore soils, as well as that of previously

published comparable incubation studies. Greater and prolonged N₂O emissions in the large-pore soils resulted from greater N₂O production, and not from the lower N₂O to N₂ conversion, as previously expected. The enhanced emissions were driven by higher microbial activity, possibly fungi, as attested by marked surge in chitinase activity. Chitinase activity in the large-pore soils increased at a greater rate and remained higher than in the small-pore soil, suggesting that the high N₂O emissions were related to faster root decomposition and microbial turnover in the former rhizosphere. Root-derived N was the main source of N₂O, especially in the large-pore soils; however, *in-situ* root decomposition also accelerated mining of SOM-N for N₂O and N₂O priming. Apparently, the location for such priming was the former rhizosphere soil in close proximity to the decaying roots. Microbial processes leading to N₂O production in the soil dominated by large pores become decoupled from the CO₂ generating microbial activities, suggesting a different group of microbes being involved in N₂O production, possibly, strategically procuring N from the root residues and the soil.

We demonstrated that the rhizosphere soil carries a strong legacy effect as it turns into a detritusphere after plant death and decomposition. Ignoring this effect by mixing root residues with destructed soil may underestimate the durations and intensities of N₂O emissions. Our study emphasized the pore architecture as a crucial factor that determines the magnitude and longevity of N₂O emission hotspots. It revealed that the role of pores in pathways of climate change can be more important than previously perceived.

Acknowledgements

- Support for this research was provided by the Great Lakes Bioenergy Research Center, U.S.
- Department of Energy, Office of Science, Office of Biological and Environmental Research
- (Award DE-SC0018409), by the National Science Foundation Long-term Ecological Research
- Program (DEB 1832042) at the Kellogg Biological Station, and by Michigan State University
- AgBioResearch, and the "RUDN University program 5-100". We appreciate the support from
- Samuel Decamp, Kevin Kahmark, and David Weed for sample analyses and related lab works.
- We also want to thank Lisa Tiemann for sharing the seed stimulation/germination protocol.

828

838

839

840

841

842

843 844

845

References

- Adler, P.R., Grosso, S.J.D. and Parton, W.J., 2007. Life-cycle assessment of net greenhouse-gas flux for bioenergy cropping systems. Ecological Applications. 17, 675-691.
- Angers, D.A. and Caron, J., 1998. Plant-induced changes in soil structure: processes and feedbacks. Biogeochemistry. 42, 55-72.
- Azam, F., Müller, C., Weiske, A., Benckiser, G. and Ottow, J., 2002. Nitrification and denitrification as sources of atmospheric nitrous oxide—role of oxidizable carbon and applied nitrogen. Biology and Fertility of Soils. 35, 54-61.
- Bardgett, R.D., Mommer, L. and De Vries, F.T., 2014. Going underground: root traits as drivers of ecosystem processes. Trends in Ecology & Evolution. 29, 692-699.
 - Bateman, E. and Baggs, E., 2005. Contributions of nitrification and denitrification to N2O emissions from soils at different water-filled pore space. Biology and Fertility of Soils. 41, 379-388.
 - Begum, N., Guppy, C., Herridge, D. and Schwenke, G., 2014. Influence of source and quality of plant residues on emissions of N2O and CO2 from a fertile, acidic Black Vertisol. Biology and Fertility of Soils. 50, 499-506.
 - Bengough, A., 2012. Water dynamics of the root zone: rhizosphere biophysics and its control on soil hydrology. Vadose Zone Journal. 11, vzj2011.0111.
- Berendsen, R.L., Pieterse, C.M. and Bakker, P.A., 2012. The rhizosphere microbiome and plant health. Trends in Plant Science. 17, 478-486.
- Bird, J.A., Herman, D.J. and Firestone, M.K., 2011. Rhizosphere priming of soil organic matter by bacterial groups in a grassland soil. Soil Biology and Biochemistry. 43, 718-725.
- Blagodatsky, S., Grote, R., Kiese, R., Werner, C. and Butterbach-Bahl, K., 2011. Modelling of microbial carbon and nitrogen turnover in soil with special emphasis on N-trace gases emission. Plant and Soil. 346, 297-330.
- Blossfeld, S., Schreiber, C.M., Liebsch, G., Kuhn, A.J. and Hinsinger, P., 2013. Quantitative imaging of rhizosphere pH and CO2 dynamics with planar optodes. Annals of Botany. 112(2), 267-276.

- Bollmann, A. and Conrad, R., 1998. Influence of O2 availability on NO and N2O release by nitrification and denitrification in soils. Global Change Biology. 4, 387-396.
- Bouckaert, L., Sleutel, S., Van Loo, D., Brabant, L., Cnudde, V., Van Hoorebeke, L., De Neve, S., 2013. Carbon mineralisation and pore size classes in undisturbed soil cores. Soil Res. 51 (1), 14–22. Haling, R.E., Tighe, M.K., Flavel, R.J., Young, I.M., 2013. Application of X-ray computed tomography to quantify fresh root decomposition in situ. Plant and Soil. 372 (1-2), 619–627.
- Bracken, C.J., Lanigan, G.J., Richards, K.G., Müller, C., Tracy, S.R., Grant, J., Krol, D.J.,
 Sheridan, H., Lynch, M.B., Grace, C. and Fritch, R., 2021. Source partitioning using N2O isotopomers and soil WFPS to establish dominant N2O production pathways from different pasture sward compositions. Science of the Total Environment. 781, 146515.
 - Braker, G. and Conrad, R., 2011. Diversity, structure, and size of N2O-producing microbial communities in soils—what matters for their functioning? Advances in Applied Microbiology. 75, 33-70.

868

869

873

874 875

876

877

878 879

882

883

884

885

886

887 888

889

- Bromand, S., Whalen, J.K., Janzen, H.H., Schjoerring, J.K. and Ellert, B., 2001. A pulselabelling method to generate 13C-enriched plant materials. Plant and Soil, 235(2): 253-257.
 - Brookes, P., Landman, A., Pruden, G. and Jenkinson, D., 1985. Chloroform fumigation and the release of soil nitrogen: a rapid direct extraction method to measure microbial biomass nitrogen in soil. Soil Biology and Biochemistry. 17, 837-842.
 - Butterbach-Bahl, K., Baggs, E.M., Dannenmann, M., Kiese, R. and Zechmeister-Boltenstern, S., 2013. Nitrous oxide emissions from soils: how well do we understand the processes and their controls? Philosophical Transactions of the Royal Society B: Biological Sciences. 368, 20130122.
- Calleja-Cabrera, J., Boter, M., Oñate-Sánchez, L. and Pernas, M., 2020. Root growth adaptation to climate change in crops. Frontiers in Plant Science. 11, 544.
 - Caplan, J.S., Giménez, D., Subroy, V., Heck, R.J., Prior, S.A., Runion, G.B. and Torbert, H.A., 2017. Nitrogen-mediated effects of elevated CO2 on intra-aggregate soil pore structure. Global Change Biology. 23, 1585-1597.
 - Carminati, A., Moradi, A.B., Vetterlein, D., Vontobel, P., Lehmann, E., Weller, U., Vogel, H.-J. and Oswald, S.E., 2010. Dynamics of soil water content in the rhizosphere. Plant and Soil. 332, 163-176.
 - Castellano, M.J., Schmidt, J.P., Kaye, J.P., Walker, C., Graham, C.B., Lin, H. and Dell, C.J., 2010. Hydrological and biogeochemical controls on the timing and magnitude of nitrous oxide flux across an agricultural landscape. Global Change Biology. 16, 2711-2720.
- Chen, H., Li, X., Hu, F. and Shi, W., 2013. Soil nitrous oxide emissions following crop residue addition: A meta-analysis. Global Change Biology. 19, 2956-2964.
- Chenu, C. and Cosentino, D., 2011. Microbial regulation of soil structural dynamics. The Architecture and Biology of Soils: Life in Inner Space. 37-70.
- Cherubini, F. and Jungmeier, G., 2010. LCA of a biorefinery concept producing bioethanol, bioenergy, and chemicals from switchgrass. The International Journal of Life Cycle Assessment. 15, 53-66.
- Daly, E.J. and Hernandez-Ramirez, G., 2020. Sources and priming of soil N2O and CO2 production: Nitrogen and simulated exudate additions. Soil Biology and Biochemistry. 149, 107942.

- Davidson, E.A., 1991. Fluxes of nitrous oxide and nitric oxide from terrestrial ecosystems.

 Microbial Production and Consumption of Greenhouse Gases: Methane, Nitrogen
 Oxides, and Halomethanes., 219-235.
- Davidson, E.A., Swank, W.T. and Perry, T.O., 1986. Distinguishing between nitrification and denitrification as sources of gaseous nitrogen production in soil. Applied and Environmental Microbiology. 52, 1280-1286.
- De Boer, W., Gerards, S., Gunnewiek, P.K. and Modderman, R., 1999. Response of the chitinolytic microbial community to chitin amendments of dune soils. Biology and Fertility of Soils, 29(2): 170-177.
- Dijkstra, F.A., Bader, N.E., Johnson, D.W. and Cheng, W., 2009. Does accelerated soil organic
 matter decomposition in the presence of plants increase plant N availability? Soil Biology
 and Biochemistry. 41, 1080-1087.
- Doane, T.A. and Horwáth, W.R., 2003. Spectrophotometric determination of nitrate with a single reagent. Analytical Letters. 36, 2713-2722.
- Doube, M., Kłosowski, M.M., Arganda-Carreras, I., Cordeliéres, F., Dougherty, R.P., Jackson,
 J., Schmid. B., Hutchinson. J,R., Shefelbine. S.J., 2010, BoneJ: free and extensible bone image analysis in ImageJ. Bone 47:1076-9.
- Duan, P., Song, Y., Li, S. and Xiong, Z., 2019. Responses of N2O production pathways and
 related functional microbes to temperature across greenhouse vegetable field soils.
 Geoderma. 355, 113904.

925

926

927

928

929

930

931

- Fan, F., Yin, C., Tang, Y., Li, Z., Song, A., Wakelin, S.A., Zou, J. and Liang, Y., 2014. Probing potential microbial coupling of carbon and nitrogen cycling during decomposition of maize residue by 13C-DNA-SIP. Soil Biology and Biochemistry. 70, 12-21.
 - Fontaine, S., Mariotti, A. and Abbadie, L., 2003. The priming effect of organic matter: a question of microbial competition? Soil Biology and Biochemistry. 35, 837-843.
 - Gaillard, V., Chenu, C., Recous, S. and Richard, G., 1999. Carbon, nitrogen and microbial gradients induced by plant residues decomposing in soil. European Journal of Soil Science. 50, 567-578.
 - Gelfand, I., Hamilton, S.K., Kravchenko, A.N., Jackson, R.D., Thelen, K.D. and Robertson, G.P., 2020. Empirical Evidence for the Potential Climate Benefits of Decarbonizing Light Vehicle Transport in the US with Bioenergy from Purpose-Grown Biomass with and without BECCS. Environmental Science & Technology. 54, 2961-2974.
- Groffman, P.M. and Tiedje, J.M., 1989. Denitrification in north temperate forest soils: spatial and temporal patterns at the landscape and seasonal scales. Soil Biology and Biochemistry. 21, 613-620.
- Groffman, P.M., Butterbach-Bahl, K., Fulweiler, R.W., Gold, A.J., Morse, J.L., Stander, E.K.,
 Tague, C., Tonitto, C. and Vidon, P., 2009. Challenges to incorporating spatially and
 temporally explicit phenomena (hotspots and hot moments) in denitrification models.
 Biogeochemistry. 93, 49-77.
- Gu, J., Nicoullaud, B., Rochette, P., Grossel, A., Hénault, C., Cellier, P. and Richard, G., 2013.
 A regional experiment suggests that soil texture is a major control of N2O emissions
 from tile-drained winter wheat fields during the fertilization period. Soil Biology and
 Biochemistry. 60, 134-141.
- Guber, A., Blagodatskaya, E., Juyal, A., Razavi, B.S., Kuzyakov, Y. and Kravchenko, A., 2021.
 Time-lapse approach: correcting deficiencies of 2D soil zymography. Soil Biology and Biochemistry. 108225.

- Guber, A., Kravchenko, A., Razavi, B.S., Uteau, D., Peth, S., Blagodatskaya, E. and Kuzyakov,
 Y., 2018. Quantitative soil zymography: mechanisms, processes of substrate and enzyme
 diffusion in porous media. Soil Biology and Biochemistry. 127, 156-167.
- Guber, A.K., Kravchenko, A.N., Razavi, B.S., Blagodatskaya, E. and Kuzyakov, Y., 2019.
 Calibration of 2-D soil zymography for correct analysis of enzyme distribution. European
 Journal of Soil Science. 70, 715-726.
- Guenet, B., Leloup, J., Raynaud, X., Bardoux, G. and Abbadie, L., 2010. Negative priming effect
 on mineralization in a soil free of vegetation for 80 years. European Journal of Soil
 Science. 61, 384-391.
 - Gupta, V.V. and Germida, J.J., 2015. Soil aggregation: Influence on microbial biomass and implications for biological processes. Soil Biology and Biochemistry. 80, A3-A9.

958

959

960

961

962 963

964

965 966

967

968

969

976

977

978 979

- Heitkötter, J. and Marschner, B., 2018. Soil zymography as a powerful tool for exploring hotspots and substrate limitation in undisturbed subsoil. Soil Biology and Biochemistry. 124, 210-217.
- Helliwell, J.R., Sturrock, C.J., Miller, A.J., Whalley, W.R. and Mooney, S.J., 2019. The role of plant species and soil condition in the structural development of the rhizosphere. Plant, Cell & Environment, 42(6): 1974-1986.
 - Herman, D.J., Firestone, M.K., Nuccio, E. and Hodge, A., 2012. Interactions between an arbuscular mycorrhizal fungus and a soil microbial community mediating litter decomposition. FEMS Microbiology Ecology. 80, 236-247.
- Hinsinger P., Plassard C., Tang C., Jaillard B., 2003. Origins of root-mediated pH changes in the rhizosphere and their responses to environmental constraints: a review. Plant and Soil. 248, 43-59.
- Hirmas, D.R., Giménez, D., Nemes, A., Kerry, R., Brunsell, N.A. and Wilson, C.J., 2018.
 Climate-induced changes in continental-scale soil macroporosity may intensify water cycle. Nature. 561, 100-103.
- Hu, X., Liu, L., Zhu, B., Du, E., Hu, X., Li, P., Zhou, Z., Ji, C., Zhu, J. and Shen, H., 2016.
 Asynchronous responses of soil carbon dioxide, nitrous oxide emissions and net nitrogen mineralization to enhanced fine root input. Soil Biology and Biochemistry. 92, 67-78.
 - Iqbal, A., Beaugrand, J., Garnier, P. and Recous, S., 2013. Tissue density determines the water storage characteristics of crop residues. Plant and Soil. 367, 285-299.
 - Jach-Smith, L.C. and Jackson, R.D., 2020. Inorganic N addition replaces N supplied to switchgrass (Panicum virgatum) by arbuscular mycorrhizal fungi. Ecological Applications. 30, e02047.
- Jin, K., White, P.J., Whalley, W.R., Shen, J. and Shi, L., 2017. Shaping an optimal soil by root—soil interaction. Trends in Plant Science. 22, 823-829.
- Juarez, S., Nunan, N., Duday, A.C., Pouteau, V., Schmidt, S., Hapca, S., Falconer, R., Otten, W.,
 Chenu, C., 2013. Effects of different soil structures on the decomposition of native and
 added organic carbon. European Journal of Soil Biology. 58, 81–90.
- Kaiser, E.-A. and Heinemeyer, O., 1996. Temporal changes in N2O-losses from two arable soils.
 Plant and Soil. 181, 57-63.
- Koebernick, N. et al., 2017. High-resolution synchrotron imaging shows that root hairs influence rhizosphere soil structure formation. New Phytologist, 216(1): 124-135.
- Keiluweit, M., Wanzek, T., Kleber, M., Nico, P. and Fendorf, S., 2017. Anaerobic microsites
 have an unaccounted role in soil carbon stabilization. Nature communications. 8, 1-10.

- 992 Khosrozadeh, S., Guber, A.K., Kravchenko, A.N., Ghaderi, N., Blagodatskaya, E., 2021. Soil 993 Oxidoreductase Zymography: Visualizing the Spatial Distribution of Peroxidases and 994 Phenol Oxidases Activity at the Root-Soil Interface. In review
- Kim, K., Guber, A., Rivers, M. and Kravchenko, A., 2020. Contribution of decomposing plant roots to N2O emissions by water absorption. Geoderma. 375, 114506.
- Kim, K., Kutlu, T., Kravchenko, A. and Guber, A., 2021. Dynamics of N2O in vicinity of plant
 residues: a microsensor approach. Plant and Soil.
- Köbke, S., Senbayram, M., Pfeiffer, B., Nacke, H. and Dittert, K., 2018. Post-harvest N2O and CO2 emissions related to plant residue incorporation of oilseed rape and barley straw depend on soil NO3-content. Soil and Tillage Research. 179, 105-113.
- Kögel-Knabner, I., Guggenberger, G., Kleber, M., Kandeler, E., Kalbitz, K., Scheu, S.,
 Eusterhues, K. and Leinweber, P., 2008. Organo-mineral associations in temperate soils:
 Integrating biology, mineralogy, and organic matter chemistry. Journal of Plant Nutrition
 and Soil Science. 171, 61-82.
- Kravchenko, A., Fry, J. and Guber, A., 2018. Water absorption capacity of soil-incorporated
 plant leaves can affect N2O emissions and soil inorganic N concentrations. Soil Biology
 and Biochemistry. 121, 113-119.
- Kravchenko, A.N. and Guber, A.K., 2017. Soil pores and their contributions to soil carbon processes. Geoderma, 287: 31-39.
- Kravchenko, A., Guber, A., Gunina, A., Dippold, M. and Kuzyakov, Y., 2021. Pore-scale view
 of microbial turnover: Combining 14C imaging, μCT and zymography after adding
 soluble carbon to soil pores of specific sizes. European Journal of Soil Science. 72, 593 607.
- Kravchenko, A., Toosi, E., Guber, A., Ostrom, N., Yu, J., Azeem, K., Rivers, M. and Robertson,
 G., 2017. Hotspots of soil N2O emission enhanced through water absorption by plant
 residue. Nature Geoscience. 10, 496-500.
- 1018 Kutlu, T., Guber, A.K., Rivers, M.L. and Kravchenko, A.N., 2018. Moisture absorption by plant residue in soil. Geoderma. 316, 47-55.
- Kuzyakov, Y., 2010. Priming effects: interactions between living and dead organic matter. Soil Biology and Biochemistry. 42, 1363-1371.
- Kuzyakov, Y. and Blagodatskaya, E., 2015. Microbial hotspots and hot moments in soil: Concept & review. Soil Biology and Biochemistry, 83, 184-199.
- Kuzyakov, Y. and Bol, R., 2006. Sources and mechanisms of priming effect induced in two grassland soils amended with slurry and sugar. Soil Biology and Biochemistry. 38, 747-1026 758.
- Kuzyakov, Y., Friedel, J. and Stahr, K., 2000. Review of mechanisms and quantification of priming effects. Soil Biology and Biochemistry. 32, 1485-1498.
- Kuzyakov Y., Razavi B.S. 2019. Rhizosphere size and shape: Temporal dynamics and spatial stationarity. Soil Biology and Biochemistry 135, 343-360.
- Leake, J.R., Donnelly, D.P. and Boddy, L., 2003. Interactions Between Ecto-mycorrhizal and
 Saprotrophic Fungi. In: M.G.A. van der Heijden and I.R. Sanders (Editors), Mycorrhizal
 Ecology. Springer Berlin Heidelberg, Berlin, Heidelberg, pp. 345-372.
- Li, H., Bölscher, T., Winnick, M., Tfaily, M.M., Cardon, Z.G. and Keiluweit, M., 2021. Simple Plant and Microbial Exudates Destabilize Mineral-Associated Organic Matter via Multiple Pathways. Environmental Science & Technology. 55, 3389-3398.

- Li, X., Sørensen, P., Olesen, J.E. and Petersen, S.O., 2016. Evidence for denitrification as main source of N2O emission from residue-amended soil. Soil Biology and Biochemistry. 92, 153-160.
- Liang, C., Jesus, E.d.C., Duncan, D.S., Quensen, J.F., Jackson, R.D., Balser, T.C. and Tiedje,
 J.M., 2016. Switchgrass rhizospheres stimulate microbial biomass but deplete microbial
 necromass in agricultural soils of the upper Midwest, USA. Soil Biology and
 Biochemistry. 94, 173-180.
- Liu, M., Chen, X., Chen, S., Li, H. and Hu, F., 2011. Resource, biological community and soil functional stability dynamics at the soil-litter interface. Acta Ecologica Sinica, 31(6): 347-352.
- Lynch, J. and Whipps, J., 1990. Substrate flow in the rhizosphere. Plant and soil, 129(1): 1-10.
- Ma, X., Razavi, B.S., Holz, M., Blagodatskaya, E. and Kuzyakov, Y., 2017. Warming increases hotspot areas of enzyme activity and shortens the duration of hot moments in the root-detritusphere. Soil Biology and Biochemistry. 107, 226-233.
- Mangalassery, S., Sjögersten, S., Sparkes, D.L., Sturrock, C.J., Mooney, S.J., 2013. The effect of soil aggregate size on pore structure and its consequence on emission of greenhouse gases. Soil and Tillage Research 132, 39-46.
- Marschner, H., Römheld, V. and Cakmak, I., 1987. Root-induced changes of nutrient availability in the rhizosphere. Journal of Plant Nutrition. 10, 1175-1184.
- Marschner, P., Marhan, S. and Kandeler, E., 2012. Microscale distribution and function of soil microorganisms in the interface between rhizosphere and detritusphere. Soil Biology and Biochemistry. 49, 174-183.
- Mašková, T. and Klimeš, A., 2020. The effect of rhizoboxes on plant growth and root: shoot biomass partitioning. Frontiers in Plant Science, 10: 1693.
- Meier, I.C., Finzi, A.C. and Phillips, R.P., 2017. Root exudates increase N availability by stimulating microbial turnover of fast-cycling N pools. Soil Biology and Biochemistry. 106, 119-128.
- Millar, N., Baggs, E.M., 2004. Chemical composition, or quality, of agroforestry residues influences N2O emissions after their addition to soil. Soil Biology and Biochemistry. 36, 935–943.
- Milliken, G.A. and Johnson, D.E., 2002. Analysis of messy data, volume III: analysis of covariance, CRC Press.
- Milliken, G.A. and Johnson, D.E., 2009. Analysis of messy data volume 1: designed experiments, CRC Press.
- Monti, A., Barbanti, L., Zatta, A. and Zegada-Lizarazu, W., 2012. The contribution of switchgrass in reducing GHG emissions. GCB Bioenergy. 4, 420-434.
- Morley, N. and Baggs, E., 2010. Carbon and oxygen controls on N2O and N2 production during nitrate reduction. Soil Biology and Biochemistry, 42(10): 1864-1871.
- Myrold, D., Elliott, L., Papendick, R. and Campbell, G., 1981. Water Potential-Water Content Characteristics of Wheat Straw. Soil Science Society of America Journal. 45, 329-333.
- Myrold, D.D. and Tiedje, J.M., 1985. Diffusional constraints on denitrification in soil. Soil Science Society of America Journal. 49, 651-657.
- Negassa, W.C. et al., 2015. Properties of soil pore space regulate pathways of plant residue decomposition and community structure of associated bacteria. PLoS one, 10(4): e0123999.

- Nguyen, C., 2003. Rhizodeposition of organic C by plants: mechanisms and controls.

 Agronomie, 23(5-6): 375-396.
- Nicolardot, B., Bouziri, L., Bastian, F. and Ranjard, L., 2007. A microcosm experiment to
 evaluate the influence of location and quality of plant residues on residue decomposition
 and genetic structure of soil microbial communities. Soil Biology and Biochemistry. 39,
 1631-1644.
- Parkin, T.B., 1987. Soil microsites as a source of denitrification variability. Soil Science Society of America Journal. 51, 1194-1199.
- Quemada, M. and Cabrera, M., 2002. Characteristic moisture curves and maximum water content of two crop residues. Plant and Soil. 238, 295-299.
- Quigley, M.Y., Negassa, W.C., Guber, A.K., Rivers, M.L. and Kravchenko, A.N., 2018.
 Influence of pore characteristics on the fate and distribution of newly added carbon.
 Frontiers in Environmental Science. 6, 51.

1097

1109

1110

- Razavi, B.S., Zarebanadkouki, M., Blagodatskaya, E. and Kuzyakov, Y., 2016. Rhizosphere shape of lentil and maize: spatial distribution of enzyme activities. Soil Biology and Biochemistry. 96, 229-237.
- Roberts, B.J., Russ, M.E. and Ostrom, N.E., 2000. Rapid and Precise Determination of the δ18O
 of Dissolved and Gaseous Dioxygen via Gas Chromatography— Isotope Ratio Mass
 Spectrometry. Environmental Science & Technology. 34, 2337-2341.
- Rohe, L., Apelt, B., Vogel, H.J., Well, R., Wu, G.M., Schlüter, S., 2021. Denitrification in soil as a function of oxygen availability at the microscale. Biogeosciences 18(3), 1185-1201.
- Roley, S.S., Duncan, D.S., Liang, D., Garoutte, A., Jackson, R.D., Tiedje, J.M. and Robertson, G.P., 2018. Associative nitrogen fixation (ANF) in switchgrass (Panicum virgatum) across a nitrogen input gradient. PloS One. 13, e0197320.
- Roman-Perez, C.C. and Hernandez-Ramirez, G., 2020. Sources and priming of N2O production across a range of moisture contents in a soil with high organic matter. Soil Biology and Biochemistry. 149, 107942.
 - Ruser, R., Flessa, H., Russow, R., Schmidt, G., Buegger, F. and Munch, J., 2006. Emission of N2O, N2 and CO2 from soil fertilized with nitrate: effect of compaction, soil moisture and rewetting. Soil Biology and Biochemistry. 38, 263-274.
- Saggar, S., Jha, N., Deslippe, J., Bolan, N.S., Luo, J., Giltrap, D.L., Kim, D.G., Zaman, M. and Tillman, R.W., 2013. Denitrification and N2O: N2 production in temperate grasslands:
 Processes, measurements, modelling and mitigating negative impacts. Science of the Total Environment, 465: 173-195.
- Salome, C., Nunan, N., Pouteau, V., Lerch, T.Z., Chenu, C., 2010. Carbon dynamics in topsoil and in subsoil may be controlled by different regulatory mechanisms. Global Change Biology. 16 (1), 416–426.
- Sanaullah, M., Razavi, B.S., Blagodatskaya, E. and Kuzyakov, Y., 2016. Spatial distribution and catalytic mechanisms of β-glucosidase activity at the root-soil interface. Biology and Fertility of Soils. 52, 505-514.
- Schaufler, G., Kitzler, B., Schindlbacher, A., Skiba, U., Sutton, M. and Zechmeister-Boltenstern, S., 2010. Greenhouse gas emissions from European soils under different land use: effects of soil moisture and temperature. European Journal of Soil Science. 61, 683-696.
- Schindelin, J., Arganda-Carreras, I., Frise, E., Kaynig, V., Longair, M., Pietzsch, T., Preibisch, S., Rueden, C., Saalfeld, S. and Schmid, B., 2012. Fiji: an open-source platform for biological-image analysis. Nature Methods. 9, 676-682.

- Schleusner, P., Lammirato, C., Tierling, J., Lebender, U. and Rütting, T., 2018. Primed N2O emission from native soil nitrogen: A 15N-tracing laboratory experiment. Journal of Plant Nutrition and Soil Science. 181, 621-627.
- Schlüter, S., Eickhorst, T. and Mueller, C.W., 2018. Correlative imaging reveals holistic view of soil microenvironments. Environmental Science & Technology. 53, 829-837.
- Schmidt, U., Thöni, H. and Kaupenjohann, M., 2000. Using a boundary line approach to analyze N2O flux data from agricultural soils. Nutrient Cycling in Agroecosystems. 57, 119-129.
- Shcherbak, I. and Robertson, G.P., 2019. Nitrous Oxide (N2O) Emissions from Subsurface Soils of Agricultural Ecosystems. Ecosystems. 22, 1650-1663.
- Shelton, D.R., Sadeghi, A.M. and McCarty, G.W., 2000. Effect of soil water content on denitrification during cover crop decomposition. Soil Science. 165, 365-371.
- Sinsabaugh, R. and Moorhead, D., 1994. Resource allocation to extracellular enzyme production: a model for nitrogen and phosphorus control of litter decomposition. Soil Biology and Biochemistry. 26, 1305-1311.
- Sinsabaugh, R., Reynolds, H. and Long, T., 2000. Rapid assay for amidohydrolase (urease) activity in environmental samples. Soil Biology and Biochemistry. 32, 2095-2097.

1145

1146 1147

1148

1149

1158

11591160

1161

- Spohn, M. and Kuzyakov, Y., 2013. Distribution of microbial-and root-derived phosphatase activities in the rhizosphere depending on P availability and C allocation—Coupling soil zymography with 14C imaging. Soil Biology and Biochemistry. 67, 106-113.
- Spohn, M. and Kuzyakov, Y., 2014. Spatial and temporal dynamics of hotspots of enzyme activity in soil as affected by living and dead roots—a soil zymography analysis. Plant and Soil. 379, 67-77.
- Sutka, R., Ostrom, N., Ostrom, P., Gandhi, H. and Breznak, J., 2003. Nitrogen isotopomer site preference of N2O produced by Nitrosomonas europaea and Methylococcus capsulatus Bath. Rapid Communications in Mass Spectrometry. 17, 738-745.
- Syakila, A. and Kroeze, C., 2011. The global nitrous oxide budget revisited. Greenhouse Gas Measurement and Management. 1, 17-26.
- Tabatabai, M., Ekenler, M. and Senwo, Z., 2010. Significance of enzyme activities in soil nitrogen mineralization. Communications in Soil Science and Plant Analysis. 41, 595-605.
 - Thilakarathna, S.K. and Hernandez-Ramirez, G., 2021a. Primings of soil organic matter and denitrification mediate the effects of moisture on nitrous oxide production. Soil Biology and Biochemistry. 108166.
 - Thilakarathna, S.K. and Hernandez-Ramirez, G., 2021b. How does management legacy, nitrogen addition, and nitrification inhibition affect soil organic matter priming and nitrous oxide production? Journal of Environmental Quality 50, 78-93.
- Tian, L., Cai, Y. and Akiyama, H., 2019. A review of indirect N2O emission factors from agricultural nitrogen leaching and runoff to update of the default IPCC values.

 Environmental Pollution. 245, 300-306.
- Toosi, E., Kravchenko, A., Guber, A. and Rivers, M., 2017. Pore characteristics regulate priming and fate of carbon from plant residue. Soil Biology and Biochemistry. 113, 219-230.
- van der Weerden, T.J., Kelliher, F.M. and de Klein, C.A., 2012. Influence of pore size distribution and soil water content on nitrous oxide emissions. Soil Research. 50, 125-135.
- Vance, E.D., Brookes, P.C. and Jenkinson, D.S., 1987. An extraction method for measuring soil microbial biomass C. Soil Biology and Biochemistry. 19, 703-707.

- 1174 Vedere, C., Gonod, L.V., Pouteau, V., Girardin, C. and Chenu, C., 2020. Spatial and temporal 1175 evolution of detritusphere hotspots at different soil moistures. Soil Biology and 1176 Biochemistry. 150, 107975.
- Velthof, G.L., Kuikman, P.J. and Oenema, O., 2002. Nitrous oxide emission from soils amended with crop residues. Nutrient cycling in agroecosystems, 62(3): 249-261.
- Wallenstein, M.D. and Burns, R.G., 2011. Ecology of Extracellular Enzyme Activities and
 Organic Matter Degradation in Soil: A Complex Community-Driven Process. Methods of
 Soil Enzymology. 9, 35-55.
- Wang, S., Sanford, G.R., Robertson, G.P., Jackson, R.D. and Thelen, K.D., 2019. Perennial
 bioenergy crop yield and quality response to nitrogen fertilization. BioEnergy Research.
 1-10.
- Weitz, A.M., Linder, E., Frolking, S., Crill, P. and Keller, M., 2001. N2O emissions from humid
 tropical agricultural soils: effects of soil moisture, texture and nitrogen availability. Soil
 Biology and Biochemistry. 33, 1077-1093.
- Witzgall, K., Vidal, A., Schubert, D.I., Höschen, C., Schweizer, S.A., Buegger, F., Pouteau, V., Chenu, C. and Mueller, C.W., 2021. Particulate organic matter as a functional soil component for persistent soil organic carbon. Nature Communications. 12, 1-10.
- Wu, J., Brookes, P. and Jenkinson, D., 1993. Formation and destruction of microbial biomass
 during the decomposition of glucose and ryegrass in soil. Soil Biology and Biochemistry.
 25, 1435-1441.
- Wu, Q., Zhang, C., Yu, Z., Zhang, J., Zhu, C., Zhao, Z., Xiong, J. and Chen, J., 2018. Effects of
 elevated CO2 and nitrogen addition on organic carbon and aggregates in soil planted with
 different rice cultivars. Plant and Soil. 432, 245-258.
- 1197 Xia, L., Lam, S.K., Wolf, B., Kiese, R., Chen, D. and Butterbach-Bahl, K., 2018. Trade-offs 1198 between soil carbon sequestration and reactive nitrogen losses under straw return in 1199 global agroecosystems. Global Change Biology. 24, 5919-5932.
- Yanai, Y. and Toyota, K., 2006. Effects of soil freeze-thaw cycles on microbial biomass and organic matter decomposition, nitrification and denitrification potential of soils, Proc. Int. Symp. of JSPS Core to Core Program between Hokkaido University and Martin Luther University Symptom of Environmental Change in Siberian Permafrost Region, Halle-Wittenberg, Eds. Hatano R and Guggenberger G, p 177-191, Hokkaido University Press, Sapporo.
- Zaman, M., Nguyen, M.L., Šimek, M., Nawaz, S., Khan, M.J., Babar, M.N. and Zaman, S.,
 2012. Emissions of nitrous oxide (N2O) and di-nitrogen (N2) from the agricultural
 landscapes, sources, sinks, and factors affecting N2O and N2 ratios. Greenhouse gases emission, measurement and management. (Ed. Guoxiang Liu). 1-32.
- Zhang, Z., Wang, W., Qi, J., Zhang, H., Tao, F. and Zhang, R., 2019. Priming effects of soil
 organic matter decomposition with addition of different carbon substrates. Journal of
 Soils and Sediments. 19, 1171-1178.

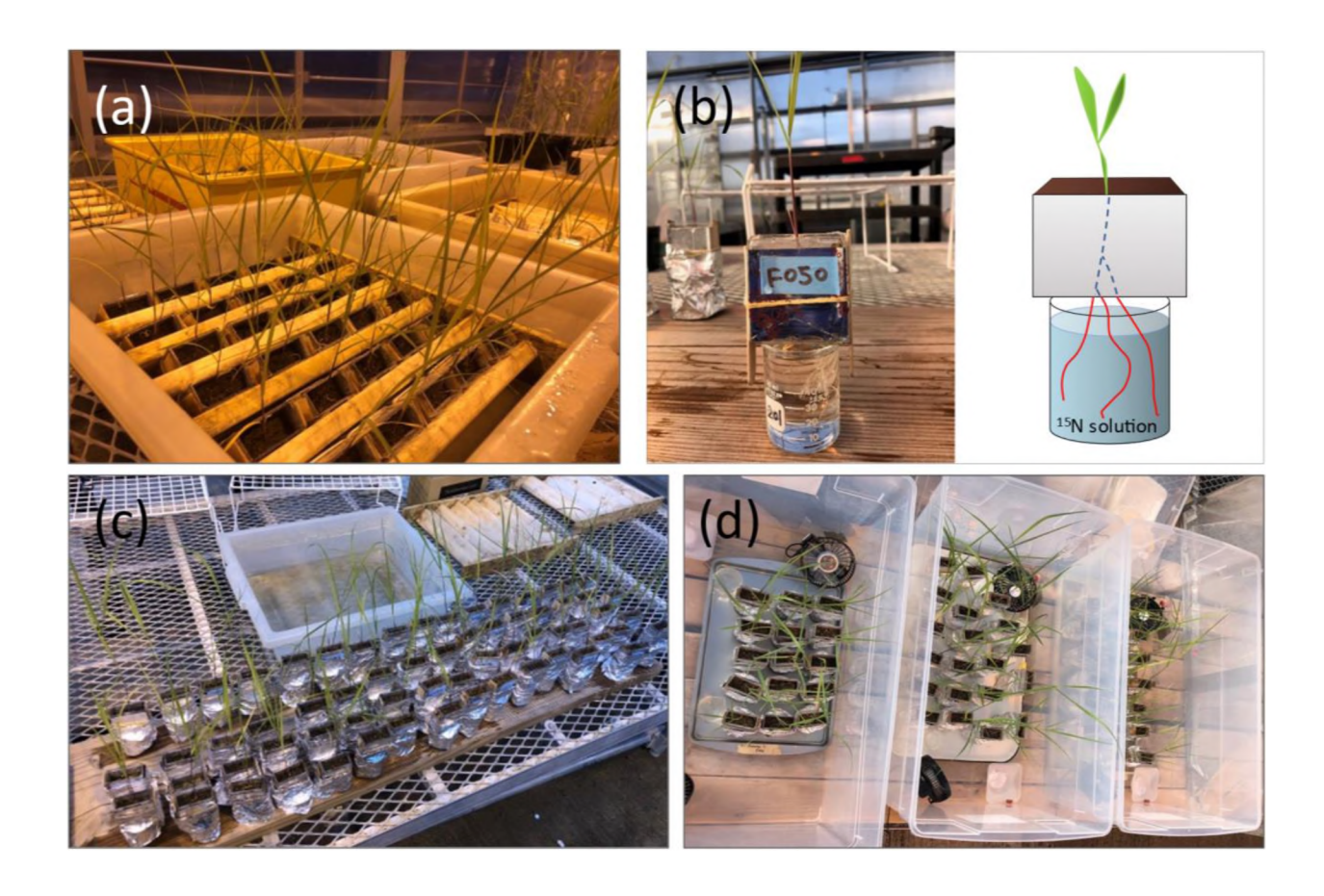


Figure 1. Switchgrass ¹⁵N and ¹³C labeling procedure. (a) Rhizoboxes placed on a rack tilted at 50° to induce root growth on the surface of the box for subsequent zymography. (b) Rhizobox placed on the beaker containing ¹⁵N Hoagland solution to label the plant without directly adding ¹⁵N to the soil. (c) Rhizoboxes and beakers sealed with aluminum foil to avoid evaporation. (d) Rhizoboxes and beakers placed in the chambers for pulse labeling the plants with ¹³CO₂.

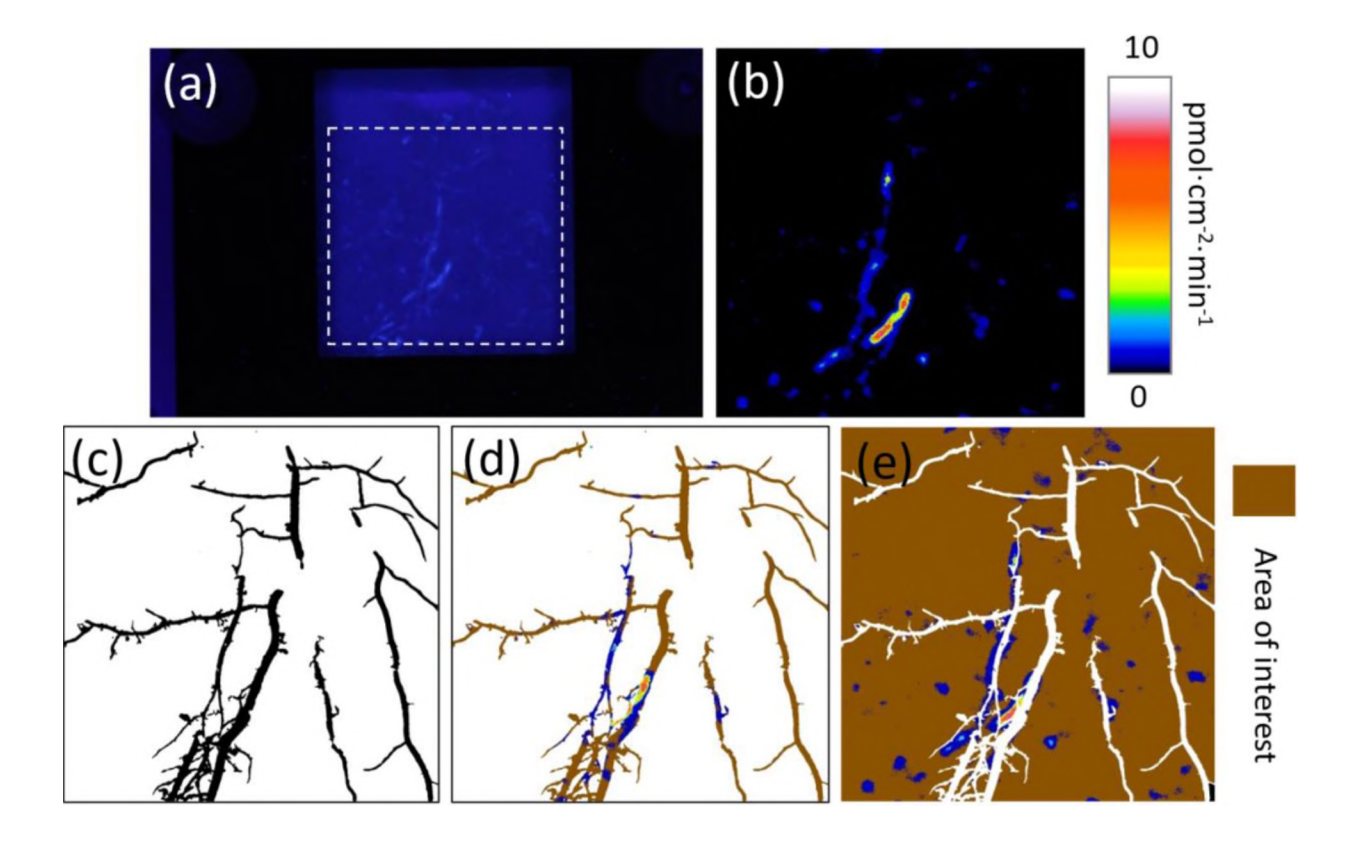


Figure 2. Illustration of zymography procedures. (a) Example of a raw image that captures the florescence developed from enzyme-substrate reaction. The white dashed box in (a) represents the region of interest used for further zymography analysis. (b) A map of enzyme activity calculated from the set of raw images taken every 5 minutes. (c) A final reference image in which black and white indicates the root and soil, respectively. (d) Chitinase activity on the surface of decomposing roots. (e) Chitinase activity on the surface of soil. In images (d) and (e), brown color represents the area of interest, and no enzyme activity was presented transparently.

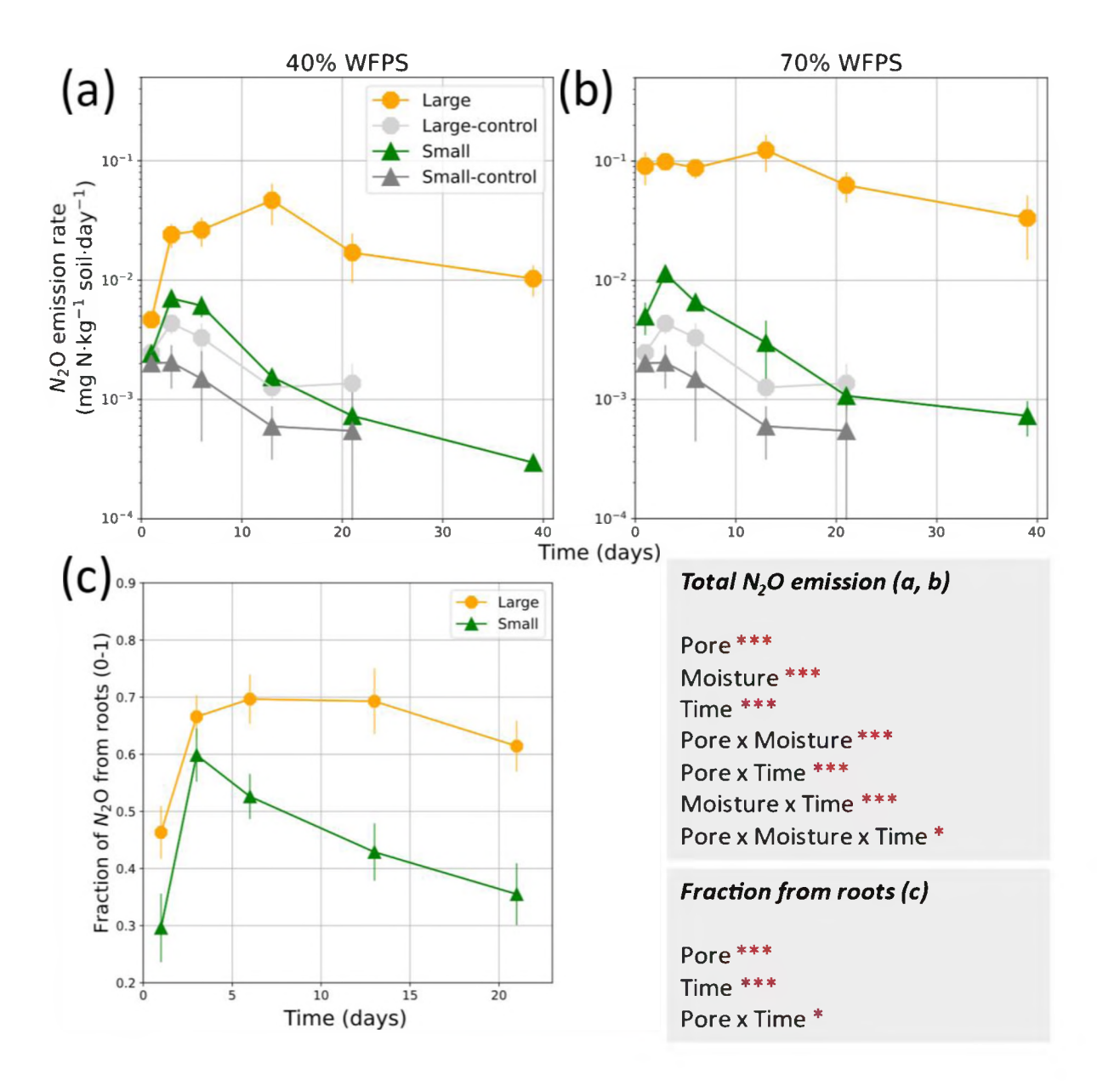


Figure 3. Dynamics of N₂O emission during the incubation: (a) total N₂O emission rate at 40% WFPS and (b) 70% WFPS; and (c) the fraction of root-derived N₂O across both WFPS treatments. Error bars are standard errors of the mean. 'Large' and 'Small' in the legends indicate the soils dominated by large (> 30 μm Ø) and small (< 10 μm Ø) pores, respectively. Controls are the rhizoboxes that were not planted and did not contain switchgrass roots. The gray box presents significant results of the factors and their interactions. Red asterisks * and *** mark statistical significance (p< 0.10 and 0.01). P-values of the factors and their interactions were presented in Table S1 (supplementary material).

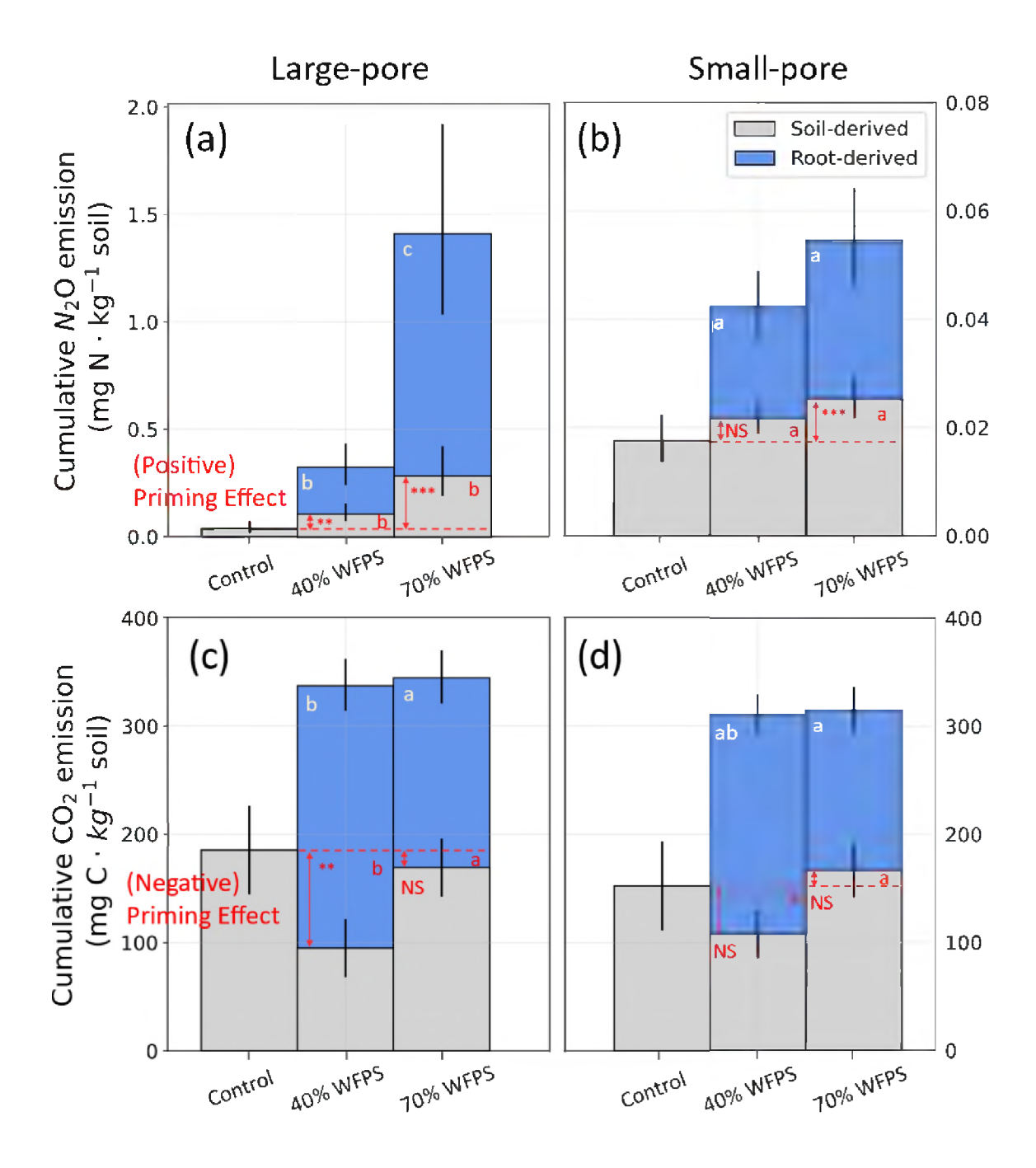


Figure 4. Cumulative N_2O emissions from the (a) large- and (b) small-pore soil; and cumulative CO_2 emission from the (c) large- and (d) small-pore soil after 21 days of incubating the rhizoboxes with ingrown switchgrass roots. Control refers to unplanted soil boxes incubated under each WFPS. Differences between soil-derived gas emission and the control gas emission (priming effect) are presented as red arrows. Red asterisks ** and *** mark the cases where the priming effect was significantly different from 0 (p< 0.05 and 0.01). NS stands for 'Not Significant'. Letters indicate the significant differences between root-derived cumulative gas emissions (white, p < 0.05) and priming effect (red, p < 0.10) at a given moisture level. Error bars are standard errors of the mean. Note the different y-axis scales between (a) and (b).

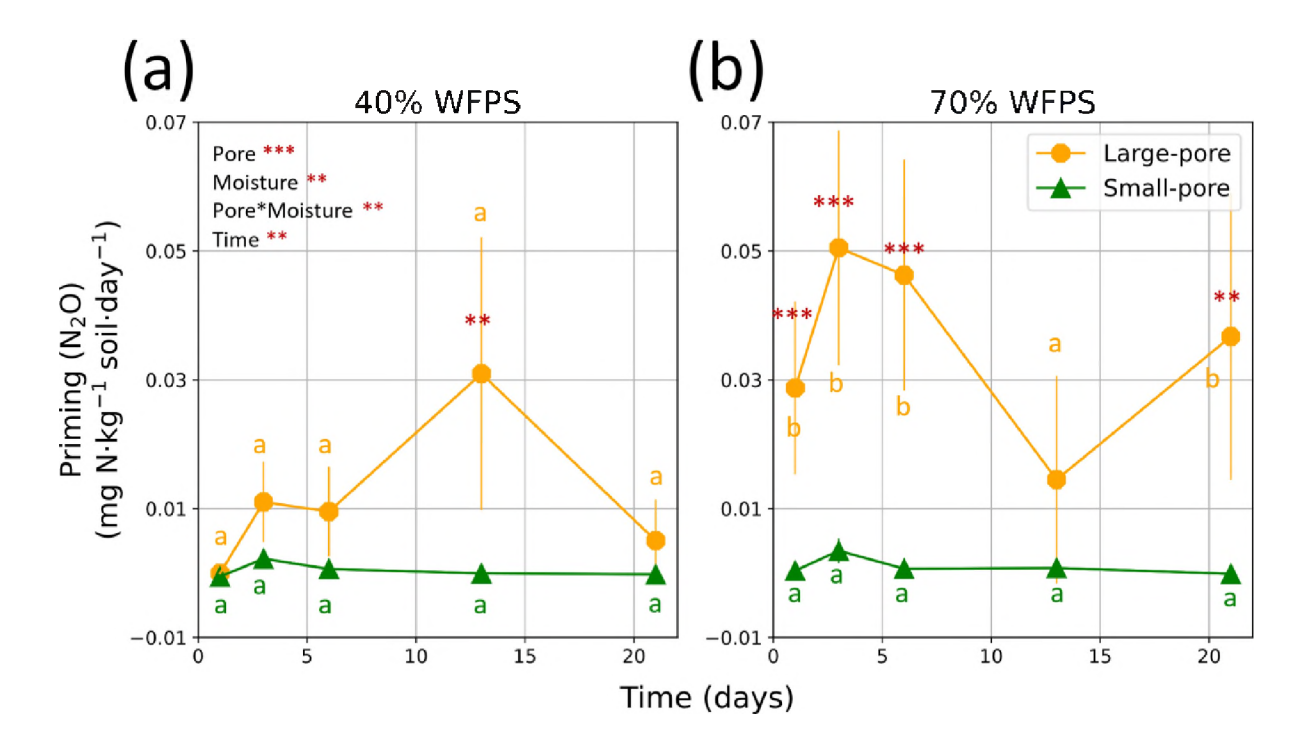


Figure 5. Dynamics of the N_2O priming effect at (a) 40% WFPS and (b) 70% WFPS in the large- and small-pore dominated soils. Red asterisks ** and *** indicate significant differences between large- and small-pores (p< 0.05 and 0.01). Letters indicate the significant differences between moisture levels at given soil materials and time (p < 0.05).

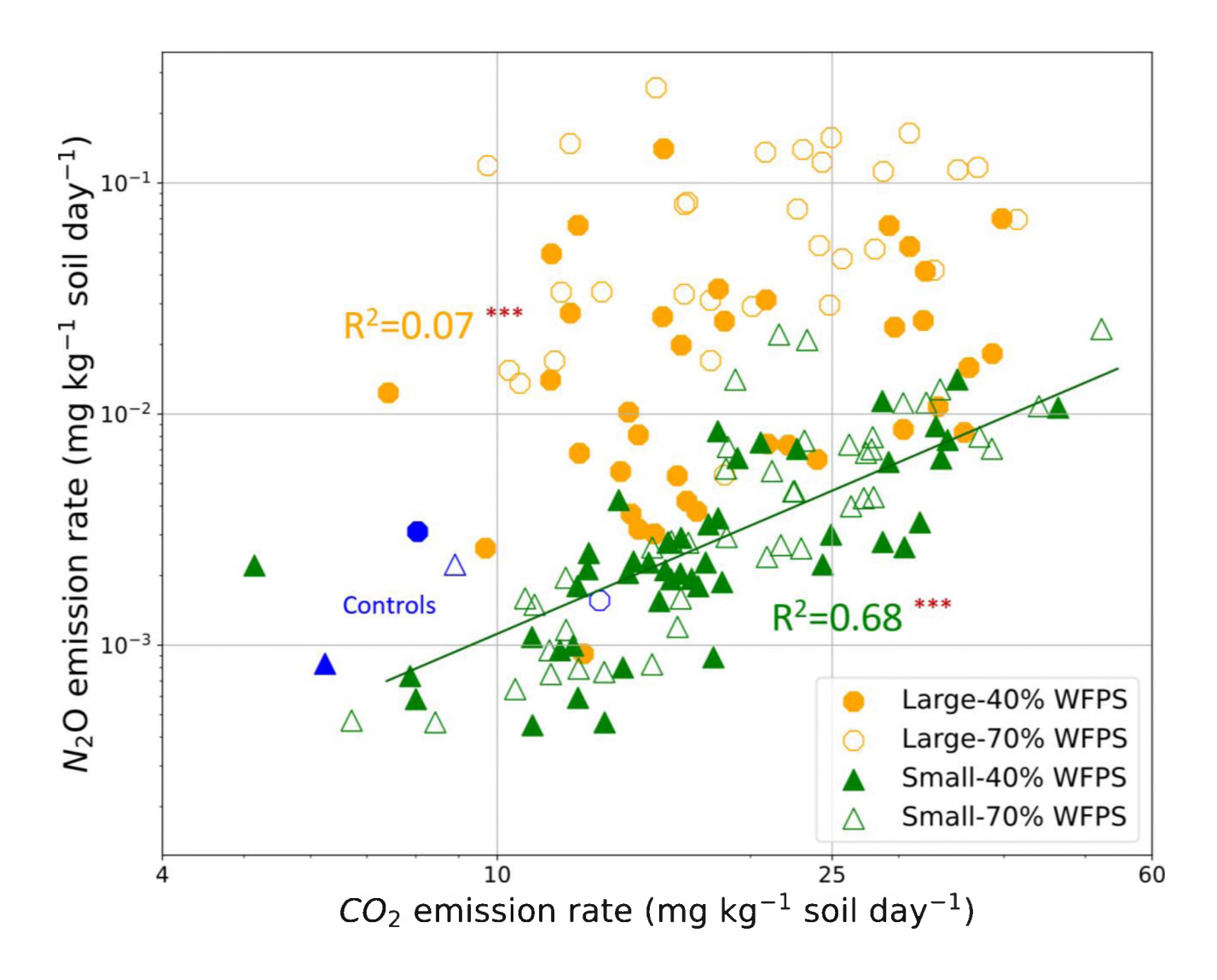


Figure 6. Relationship between total CO_2 and total N_2O emission rates in the two studied soils and moisture levels. Regression line of small-pore dominated soils was presented in green. Blue plots present the average emission rates of the unplanted controls. R^2 was reported separately for large-pore and small-pore soils (p< 0.01). Regression slope from the large pores was not presented due to low R^2 .

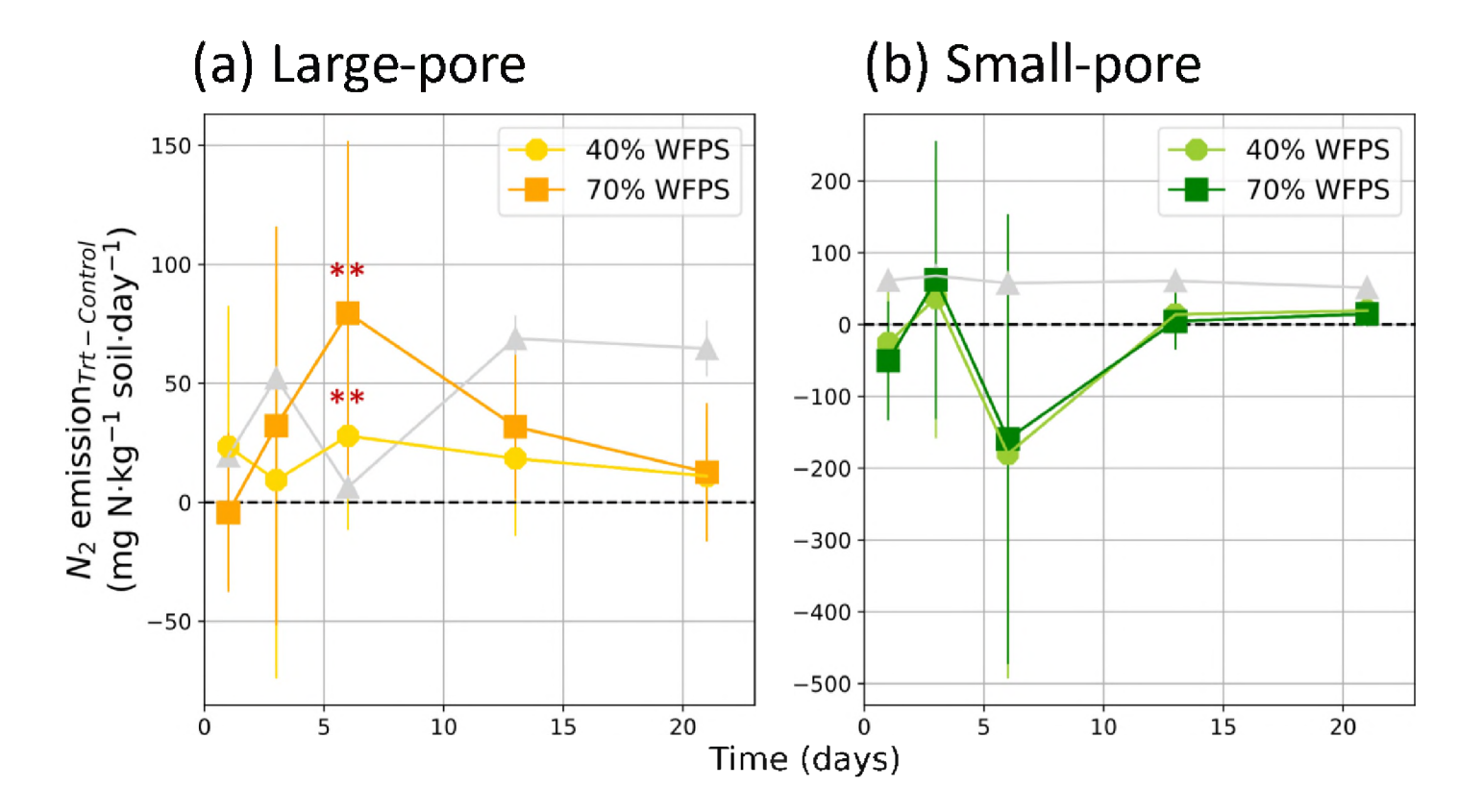


Figure 7. Dynamics of N_2 emission during the root decomposition in (a) large-pore soils and (b) small-pore soils. Shown are the differences between the planted soil and soil without plants (control). Asterisks ** mark the cases where the difference between the treatment and the control were greater than zero (p< 0.05). Error bars are standard errors of the mean. Gray lines show the actual N_2 emission (average of the two moisture levels) from planted soils.

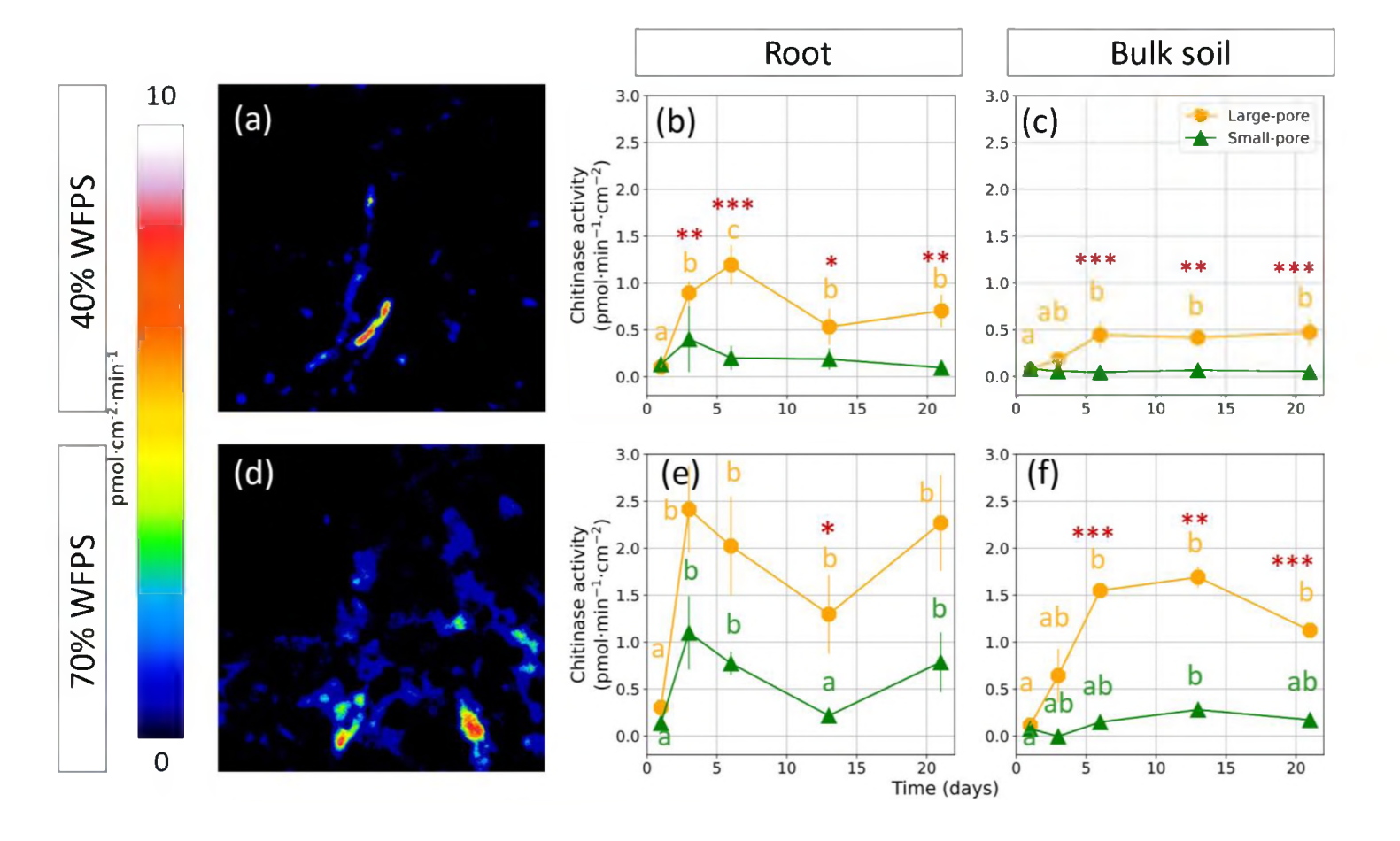


Figure 8. Dynamics of chitinase activity on root and soil surfaces in the large- and small-pore dominated soils at the two studied soil moisture levels. Example zymograms are shown in (a) and (d); root chitinase activity in (b) and (e), and soil chitinase activity in (c) and (f) for 40% and 70% WFPS, respectively. Asterisks *, **, and *** indicate the significant differences between the two soils at a given day of incubation and moisture content, at significance levels of 0.1, 0.05, and 0.01, respectively. The letters mark differences between time (incubation day) within given soil and moisture. Error bars are standard errors of the mean.

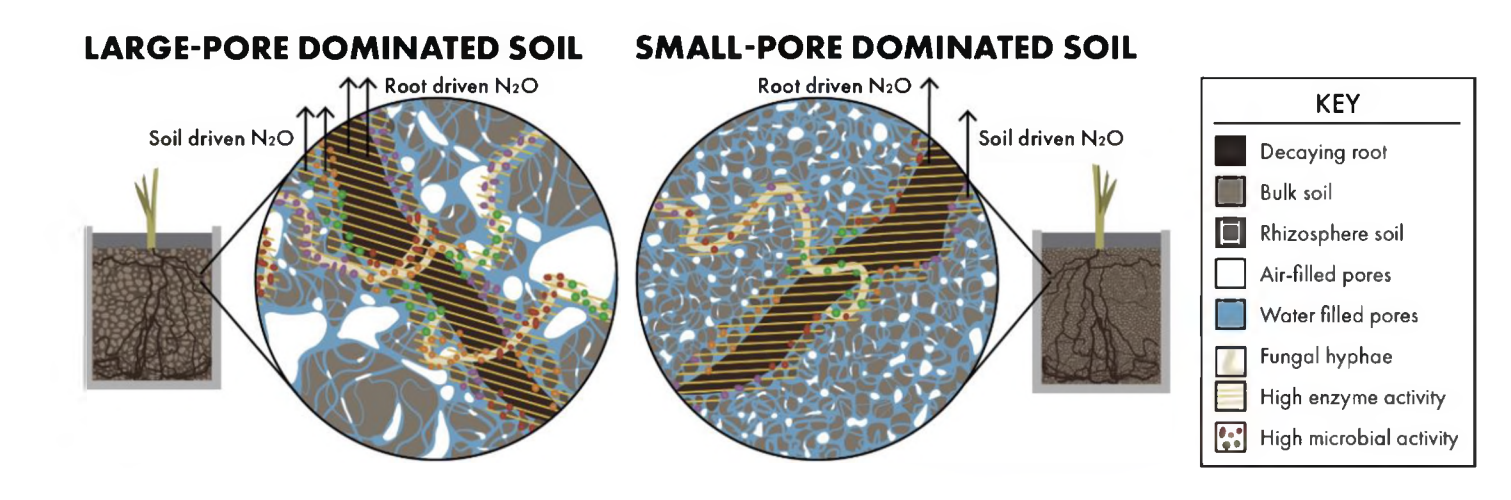


Figure 9. Conceptual model of N_2O emission drivers in the microenvironments around decaying plant roots in the soils dominated by large (>30 μm) (left) and small (<10 μm) (right) pores. The large-pore dominated soil has higher fungal growth, enzyme activity, and microbial activity near the decomposing roots. This leads to faster root decomposition and positive priming of inherent SOM, followed by greater amounts of both root-driven and soil-driven organic materials becoming available as substrates for N_2O production. The sponge effect (water absorption by decaying roots) is also more prominent in the large-pore dominated soil because of its lower water retention. Anoxic conditions within the decaying roots and in immediate detritusphere are optimal for denitrification increasing both root-derived and soil-derived N_2O production. The produced N_2O is the subject of fast emission due to atmosphere-connected large pores in close proximity to decomposing roots. The small-pore dominated soil has relatively lower fungal growth, enzyme activity, and microbial activity near the decomposing roots. Along with a less pronounced sponge effect, it creates less favorable condition for denitrification, and thus, has lower less root-derived and soil-derived N_2O production.

Table 1. C and N characteristics of soil and roots after plant growth and labeling

Switchgrass roots	Large-pore	Small-pore
Total C (mg C kg ⁻¹ dry matter)	446 (26.5)	444 (24.7)
Total N (mg N kg ⁻¹ dry matter)	29.7 (10.3)	28.8 (9.7)
Atom% ¹³ C	1.61 (0.31)	1.63 (0.29)
Atom% ¹⁵ N	8.83 (1.04)	9.10 (0.74)

Soil after plant growth	Large-pore	Small-pore
Total C (mg C kg ⁻¹ soil)	11.1 (0.4)	11.2 (0.02)
Total N (mg N kg ⁻¹ soil)	1.16 (0.03)	1.17 (0.03)
NH ₄ ⁺ (mg N kg ⁻¹ soil)	5.36 (1.08)	3.68 (1.46)
NO ₃ - (mg N kg -1 soil)	0.23 (0.10)	0.43 (0.25)
Atom% ¹³ C	1.09 (0.00)	1.09 (0.00)
Atom% ¹⁵ N	0.43 (0.02)	0.42 (0.03)
Microbial Biomass C (mg C kg-1 soil)	384° (45)	571 ^b (44)

- Standard deviations in parenthesis.
- Letters indicate significant differences between large- and small-pore soils (p< 0.05).